Geol. Mag. **151** (*5*), *2014, pp. 938–955.* © *Cambridge University Press 2014*
doi:10.1017/S0016756813000988

Smithian shoreline migrations and depositional settings in Timpoweap Canyon (Early Triassic, Utah, USA)

NICOLAS OLIVIER*,†, ARNAUD BRAYARD‡, EMMANUEL FARA‡, KEVIN G. BYLUND§, JAMES F. JENKS¶, EMMANUELLE VENNIN‡, DANIEL A. STEPHEN§ & GILLES ESCARGUEL*

*Laboratoire de Géologie de Lyon, Terre, Planètes, Environnement, UMR CNRS 5276, Université Lyon 1, 69622 Villeurbanne cedex, France
‡UMR CNRS 6282 Biogéosciences, Université de Bourgogne, 6 boulevard Gabriel, 21000 Dijon, France
§140 South 700 East, Spanish Fork, Utah 84660, USA
¶1134 Johnson Ridge Lane, West Jordan, Utah 84084, USA
§Department of Earth Science, Utah Valley University, 800 West University Parkway, Orem, Utah 84058, USA

(*Received* 10 June 2013; *accepted* 31 October 2013; *first published online* 17 January 2014)

Abstract – In Timpoweap Canyon near Hurricane (Utah, USA), spectacular outcrop conditions of Early Triassic rocks document the geometric relationships between a massive Smithian fenestral-microbial unit and underlying, lateral and overlying sedimentary units. This allows us to reconstruct the evolution of depositional environments and high-frequency relative sea-level fluctuations in the studied area. Depositional environments evolved from a coastal plain with continental deposits to peritidal settings with fenestral-microbial limestones, which are overlain by intertidal to shallow subtidal marine bioclastic limestones. This transgressive trend of a large-scale depositional sequence marks a long-term sea-level rise that is identified worldwide after the Permian–Triassic boundary. The fenestral-microbial sediments were deposited at the transition between continental settings (with terrigenous deposits) and shallow subtidal marine environments (with bioturbated and bioclastic limestones). Such a lateral zonation questions the interpretation of microbial deposits as anachronistic and disaster facies in the western USA basin. The depositional setting may have triggered the distribution of microbial deposits and contemporaneous marine biota. The fenestral-microbial unit is truncated by an erosional surface reflecting a drop in relative sea level at the scale of a medium depositional sequence. The local inherited topography allowed the recording of small-scale sequences characterized by clinoforms and short-distance lateral facies changes. Stratal stacking pattern and surface geometries allow the reconstruction of relative sea-level fluctuations and tracking of shoreline migrations. The stacking pattern of these small-scale sequences and the amplitude of corresponding high-frequency sea-level fluctuations are consistent with climatic control. Large- and medium-scale sequences suggest a regional tectonic control.

Keywords: Early Triassic, Smithian, SW Utah, relative sea level, shoreline migrations, microbialites, depositional environments.

1. Introduction

The biotic recovery after the end-Permian mass extinction is certainly not a synchronous event in all areas because its record strongly depends on the type of depositional setting (Pruss *et al.* 2006; Beatty, Zonneveld & Henderson, 2008; Zonneveld, Gingras & Beatty, 2010; Mata & Bottjer, 2011). Among the various Early Triassic marine environments, the nature of the sedimentation and putative fossil record were controlled by sea-level changes (Heydari *et al.* 2003; Weidlich, 2007). The Triassic is marked by a global long-term rise in sea level with several second- and third-order transgressive-regressive sequences that can be identified in different localities throughout the world (Haq, Hardenbol & Vail, 1987; Hallam & Wignall, 1999; Haq & Al-Qahtani, 2005). In SW Utah, the Lower Triassic sedimentary succession records three third-order transgressive-regressive cycles that originated in the Griesbachian, Smithian and earliest middle Spathian (Embry, 1997; Paull & Paull, 1997). If such long-term sea-level changes potentially controlled the evolution of the Triassic marine biota (Konstantinov, 2008; Ruban, 2008; Kelley *et al.* 2013), higher-frequency sea-level fluctuations also impacted the distribution and record of the benthic marine faunas in the aftermath of the end-Permian mass extinction (Mata & Bottjer, 2011). Although high-frequency sea-level changes are suspected in several Lower Triassic sedimentary successions (Lucas, Krainer & Milner, 2007; Chen, Fraiser & Bolton, 2012; Wu *et al.* 2012), they are rarely studied in detail because they cannot be easily dated and correlated (Embry, 1997). The nature and influence of high-frequency relative sea-level changes on the Early Triassic marine biota distribution and its record are therefore still poorly known (Yang & Lehrmann, 2003).

†Author for correspondence: Nicolas.Olivier@univ-lyon1.fr

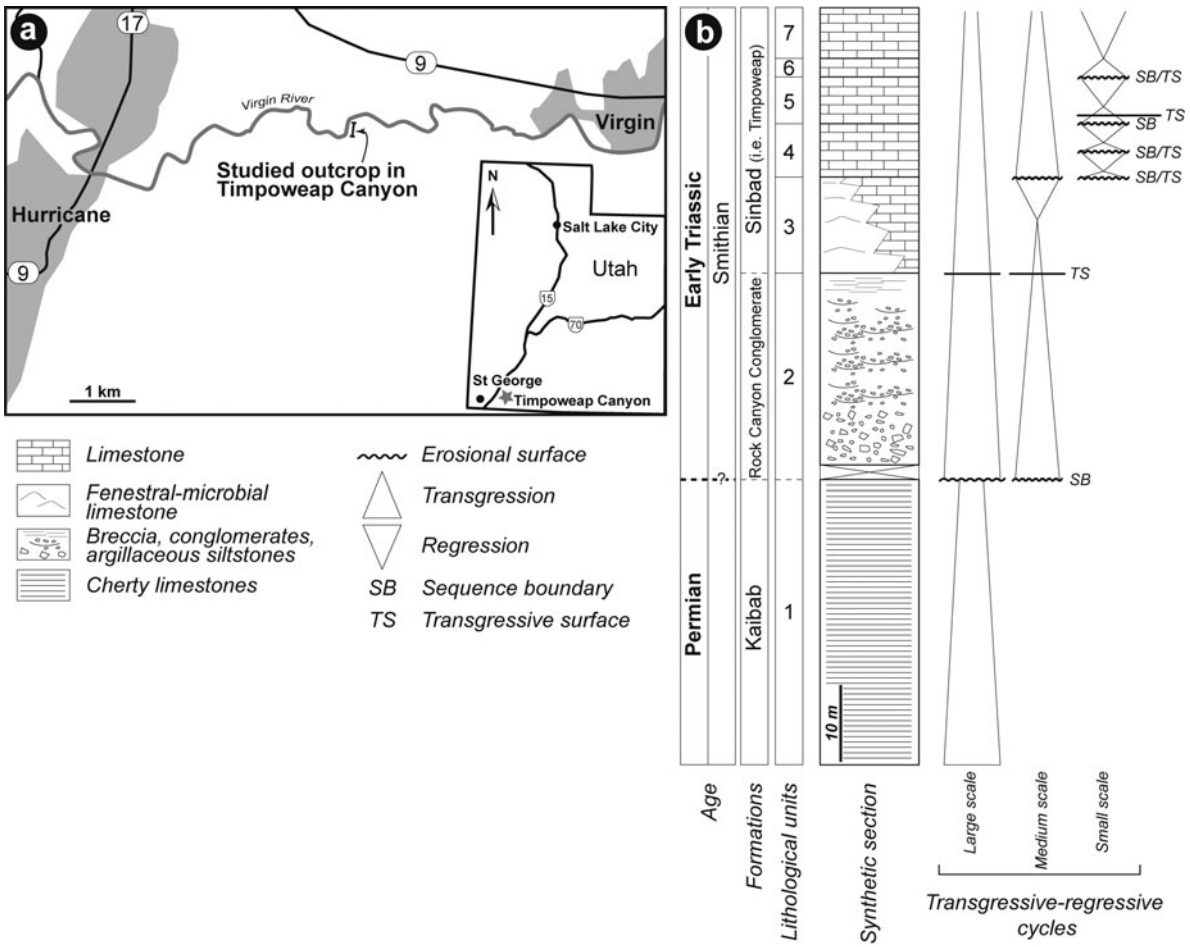

Figure 1. (a) Geographic location of Timpoweap Canyon in SW Utah. (b) Synthetic observed lithological succession with interpreted transgressive-regressive sequences.

During Early Triassic time, the Sonoma Foreland Basin of western USA was a place of continental and marginal marine sedimentation (McKee, 1954; Blakey, 1974, 1977; Collinson, Kendal & Marcantel, 1976). In SW Utah, the lowermost Lower Triassic stratigraphic unit belonging to the Thaynes Group (*sensu* Lucas, Krainer & Milner, 2007) is well exposed in Timpoweap Canyon near Hurricane, SW of Zion National Park (Gregory, 1950; Blakey, 1979; Nielson, 1991). Blakey (1979) suggested that the Timpoweap Member was deposited in a transitional area between continental and marine settings. Lucas, Krainer & Milner (2007) illustrated the type section of the Timpoweap Member (correlative of the Sinbad Formation of SE Utah) in Timpoweap Canyon. Although these authors demonstrated a general sea-level rise during Early Triassic time, they only suspected higher-frequency sea-level changes. The present study is a detailed analysis of an exceptional outcrop in Timpoweap Canyon that allows the illustration of high-frequency depositional sequences. The objectives of this paper are to (1) reconstruct the evolution of the depositional settings; (2) highlight high-frequency sea-level changes and shoreline migrations; and (3) discuss their potential origin and influence on the distribution and record of marine organisms.

2. Geological framework

The study area is located in Washington County (SW Utah, USA), *c*. 30 km NE of St George (Fig. 1a). Directly south of the road that connects Hurricane to Virgin, the Timpoweap Canyon of the Virgin River reveals an impressive Permian–Triassic sedimentary succession (Blakey, 1979; Nielson, 1991). The river gorge, which ranges up to 120 m in depth, exposes the Late Permian Harrisburg Member of the Kaibab Formation, which is overlain by the Triassic Timpoweap Member of the Moenkopi Formation (Stewart, Poole & Wilson, 1972; Blakey, 1979; Fig. 1b) or Thaynes Group (*sensu* Lucas, Krainer & Milner, 2007). Regionally, the Kaibab Formation displays an upper contact that corresponds to an erosional unconformity (Jenson, 1986), which reveals a residual karst topography (Blakey, 1979). At most locations, erosion reaches a stratigraphic unit of the Harrisburg Member made of dolomitized fossiliferous limestones that grade upwards into chert and weather to form a cliff (Nielson, 1991). Overlying the deposits of the Kaibab Formation is a laterally discontinuous unit made of breccia and conglomerates initially defined by Reeside & Bassler (1922) as the Rock Canyon Conglomerate Member. In the literature, this lithostratigraphic unit is placed

https://doi.org/10.1017/S0016756813000988 Published online by Cambridge University Press

alternatively in the Kaibab Formation (Gregory, 1950) or in the Moenkopi Formation (Reeside & Bassler, 1922; Blakey, 1979). The occurrence of conglomerates in both the Harrisburg and Timpoweap Members may explain the difficulty in delimiting the stratigraphic position of these deposits (Blakey, 1979). Gregory (1950) assumed that the Rock Canyon Conglomeratic Member was equivalent in part to the Harrisburg Member of the Kaibab Formation and proposed that the term be abandoned. Alternatively, Nielson (1991) proposed that the Rock Canyon Conglomerate should be considered as a separate Upper Permian – Lower Triassic formation. However, there is a facies gradation between the Rock Canyon Conglomerate and the limestones of the Timpoweap Member (Nielson, 1991). Such a gradation suggests that the conglomeratic deposits and overlying limestones belong to the same stratigraphic unit. The Timpoweap Member is therefore the first member of the Moenkopi Formation and corresponds to a lithologically variable unit composed mainly of sandy limestone to sandstones or siltstones, massive to thick-bedded grey limestone and chert pebble conglomerate lying above Permian rocks (Gregory, 1950; Stewart, Poole & Wilson, 1972; Blakey, 1979; Nielson, 1991). More recently, Goodspeed & Lucas (2007) and Lucas, Krainer & Milner (2007) amended the regional stratigraphic nomenclature and assigned the Sinbad and Moenkopi to formation- and group-rank units, respectively. They also restricted the Moenkopi Group to continental deposits (e.g. Rock Canyon Conglomerate and Lower Red formations) and the Thaynes Group to marine deposits (e.g. Sinbad and Virgin formations). Although still under debate, such nomenclature was recently followed by Hofmann *et al.* (2013) and Zatoń, Taylor & Vinn (2013) and is retained in this work. Moreover, Lucas, Krainer & Milner (2007) considered the Timpoweap Member as a correlative and junior synonym of the Smithian Sinbad Formation.

The Sonoma Foreland Basin of the western USA was located at a near-equatorial position in eastern Panthalassa during the Early Triassic. Smithian marine outcrops are widely distributed within a large area covering Wyoming, Idaho, Utah and Nevada (Goodspeed & Lucas, 2007). They generally contain abundant fossils and a detailed regional biostratigraphic ammonoid-based zonation has been recently proposed for this substage (Brayard *et al.* 2013). In the White Hills, the lower Spathian Virgin Formation is in disconformable contact with the Harrisburg Member, indicating that the youngest Permian–Triassic palaeogeographic highs were located west of St George (Jenson, 1986; Nielson, 1991). A previous facies analysis of deposits of the Smithian Sinbad Limestone (i.e. Timpoweap) Formation suggested that they were deposited along the shoreline of the seaway parallel to the present Hurricane Cliffs, and that the open sea was to the east (Blakey, 1979).

The Kaibab Formation in the region of Virgin is Permian in age, whereas the overlying Thaynes Group is largely Smithian and Spathian based on several index ammonoid occurrences (e.g. *Meekoceras*, *Anasibirites*, *Tirolites* and possibly *Columbites*; Stewart, Poole & Wilson, 1972; Jenson, 1986; Lucas, Krainer & Milner, 2007; Hofmann *et al.* 2013). The Smithian *Meekoceras gracilitatis* and *Anasibirites kingianus* zones were also assumed to be locally present in the Sinbad Formation (i.e. Timpoweap Member of Stewart, Poole & Wilson, 1972) of Timpoweap Canyon. The top of Timpoweap Canyon corresponds to the late Smithian *Anasibirites kingianus* zone. Dating of the uppermost units of the canyon by means of conodonts also indicated a late Smithian age (abundant ellisonids; see also Lucas, Krainer & Milner, 2007). Dating of underlying units (i.e. microbial limestones of the Sinbad Formation; Fig. 1b) is difficult as conodonts are rare and fragmentary, but one ammonoid (*Owenites* sp.) gives a middle Smithian age for the deposits just above the fenestral-microbial limestone unit. Lithological and biostratigraphical correlations of the Timpoweap Canyon succession with neighbouring Smithian outcrops near Cedar City and Kanarraville is consistent with a middle Smithian age for the limestones of the base of the Sinbad Formation (Brayard *et al.* 2013).

3. Lithological units

The studied area in Timpoweap Canyon corresponds to a N–S cliff that ranges up to *c.* 80 m in depth and *c.* 300 m in length (Figs 1a, 2a, b). Stratigraphically, the succession exposed in this cliff can be subdivided into seven lithological units (Fig. 1b). The first unit corresponds to the Permian limestones of the Kaibab Formation, while the second corresponds to sedimentary deposits of the Rock Canyon Conglomerate Formation and the last five units correspond to limestone deposits of the Smithian Sinbad Formation (Lucas, Krainer & Milner, 2007). At the uppermost part of the cliff it is not possible to observe the contact with the overlying red siltstones and fine sandstones of the Spathian Lower Red Formation, which are present in the lectostratotype section (Lucas, Krainer & Milner, 2007). These lithological units are described below according to their facies, stacking pattern and main stratigraphic surfaces.

3.a. Lithological unit 1

Even although it is beyond the scope of this study, lithological unit 1 is visible at the base of the gorge of the Virgin River and corresponds to the Permian limestones of the Kaibab Formation. Lucas, Krainer & Milner (2007) gave a detailed description of the Kaibab Formation in the lectostratotype section of Timpoweap Canyon. It consists of silicified and recrystallized limestones (including only rare ostracods and brachiopods) associated with chert layers. In the study area, well-bedded deposits of this first lithological unit display abundant silicified burrows that reflect an intense infaunal activity. The contact with the overlying

https://doi.org/10.1017/S0016756813000988 Published online by Cambridge University Press

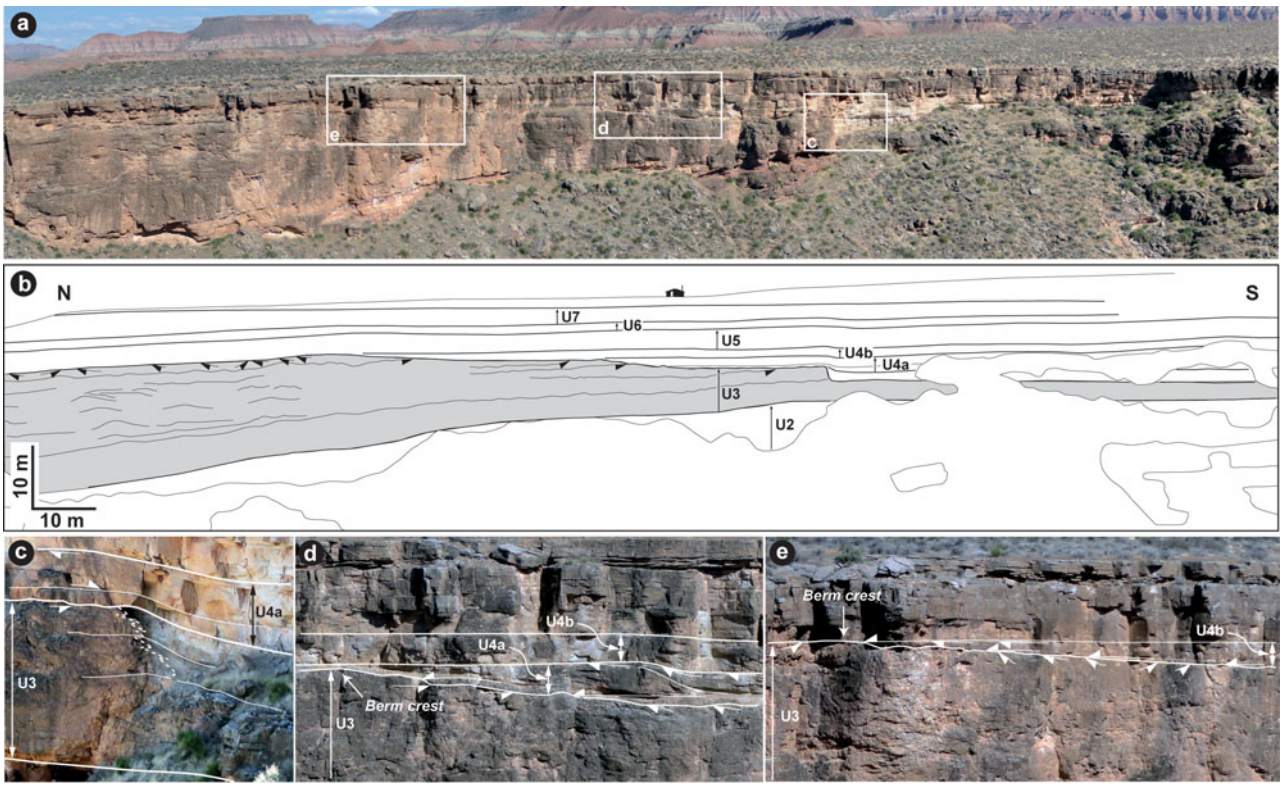

Figure 2. (Colour online) (a) Photograph and (b) line drawing of the main stratigraphic units (U2–U7) at Timpoweap Canyon. (c–e) Close-ups of some stratigraphic architectures. (c) Dashed line represents lateral facies variation between microbial-fenestral limestones and dolomudstones (lithological unit 3); first bed of lithological unit 4 onlaps on the truncation surface at the top of lithological unit 3. Small black and white arrows: stratal terminations. (d) Truncation at the top of lithological unit 3 and high-angle clinoforms of the upper wedge (subunit 4a). (e) Truncated upper part of lithological unit 3 and high-angle clinoforms (subunit 4b).

lithological unit was not observed due to vegetation cover and recent colluvium. However, this contact is regionally well known and corresponds to an erosional unconformity with a residual karst topography (Blakey, 1979; Jenson, 1986).

3.b. Lithological unit 2

Lithological unit 2 corresponds to the Rock Canyon Conglomerate Formation and can be subdivided into three subunits. A multi-metre-thick chert breccia is observed in the lowermost part of lithological unit 2. This subunit is composed of reworked, angular chert clasts up to 20 cm in diameter (Figs 1b, 3a). No sedimentary structures or clast organization were observed and clasts are embedded in an abundant matrix of coarse-grained sandstone. Overlying this breccia subunit is a multi-metre-thick conglomerate subunit made of well-rounded to subangular chert clasts. These deposits display low-angle cross-bedding and lateral accretion structures (Figs 1b, 3b). The uppermost part of lithological unit 2 displays a decimetre- to metre-thick interval of red mudstone to siltstone with sparse chert clasts (Figs 1b, 3c). In this third subunit, clasts are small (up to 2 cm in diameter) and well rounded. Silty lamina display small asymmetrical ripples. This last subunit shows lateral thickness changes and can be absent locally.

3.c. Lithological unit 3

The base of lithological unit 3 shows abundant cherty exotic clasts that gradually decrease in abundance in the first few metres of the unit (Fig. 3d). This indicates that the transition with lithological unit 2 reflects a facies gradation (as observed by Nielson, 1991) rather than a sharp surface (as suggested by Lucas, Krainer & Milner, 2007). Lithological unit 3 also displays lateral facies variations. A first facies corresponds to a massive fenestral-microbial limestone interval in the northernmost part of the studied area (Fig. 2a, b). At the outcrop scale, several undulated surfaces can be laterally followed over several tens of metres, suggesting a stratified unit. These surfaces underline the presence of metre-scale patches (Figs 1b, 2b, 4a, b). This fenestral-microbial limestone interval has an upper truncation surface that gently dips to the south (Fig. 2). Two main subfacies comprise these fenestral-microbial limestones. The first subfacies is a fenestral packstone/bindstone with laminoid fenestrae, peloids, stromatolites, cortoids and micritic ooids (Fig. 4c). Its fauna is sparse, with some ostracods, gastropods and bivalve fragments. Very rare and poorly preserved meshworks of spicules suggest the presence of putative siliceous sponges. A second subfacies can be assimilated to a pisoid biocemenstone. In this subfacies, particularly large fenestrae display domal or columnar stromatolites with upward, lateral and downward growth

https://doi.org/10.1017/S0016756813000988 Published online by Cambridge University Press

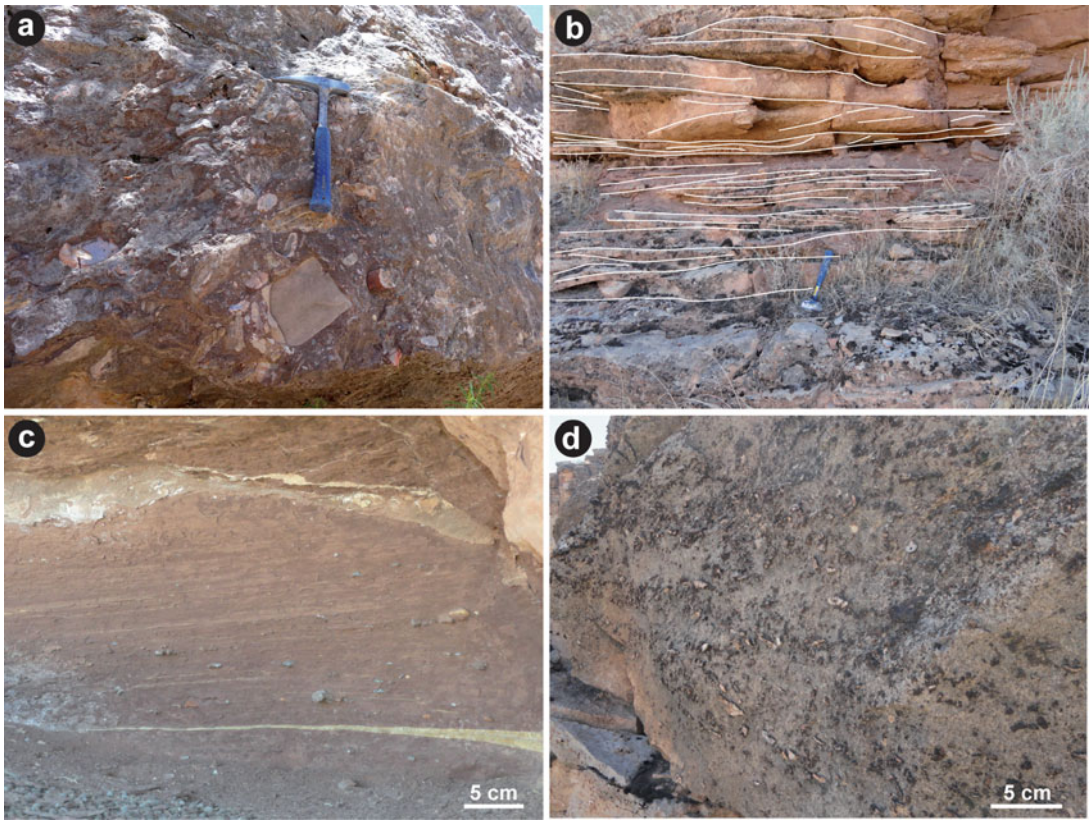

Figure 3. (Colour online) Outcrop close-up of depositional facies of lithological unit 2 and the base of lithological unit 3 at Timpoweap Canyon: (a) breccia (see hammer for scale); (b) conglomerate (see hammer for scale); (c) red sandstone; and (d) basal part of the fenestral-microbial limestones of lithological unit 3 (note the abundant extraclasts).

directions (Fig. 4d). Other large voids are unfilled by a succession of sparry carbonate cements and micritic crusts (Fig. 4e). Some domal micritic crusts display laminated sheets (Fig. 4f). Micrite or cement crusts coat various grains (Fig. 4g). Meniscus cements occurred between pisoids (Fig. 4h). There are also subrounded to rounded aggregates and locally some muddy breccias. Subrounded and poorly sorted grains of detrital quartz are abundant in the first basal metre of fenestral-microbial unit 3, but they are rare in the rest of the unit.

Lithological unit 3 displays the first N–S lateral facies variation between fenestral-microbial limestones and a dolomudstone (Figs 5a, 6a). The contemporaneity of these two facies belts is marked by the lateral continuity of some bed surfaces (Fig. 2c). The dolomudstone facies records a sparse fauna consisting of serpulids, bivalves and echinoderm plates (Fig. 5b). Quartz grains are relatively rare. The uppermost part of lithological unit 3 made of fenestral-microbial limestones is marked by a truncated surface. Laterally, the dolomudstone facies is also truncated and evolves in its uppermost part toward a subfacies that becomes rich in pisoids (Fig. 5c). A third facies is observed in lithological unit 3 in the southernmost part of the studied cliff and laterally to the dolomudstone facies. It corresponds to a bioturbated limestone with a wackestone (locally packstone) texture (Fig. 6). Associated with peloids and rare micritic ooids, the fauna is represented by gastropods, serpulids, bivalves and echinoderm plates. Quartz grains are present to common, rounded and moderately to poorly sorted.

3.d. Lithological unit 4

Lithological unit 4 is subdivided into two comparable subunits (4a and 4b), both of which display vertical and lateral facies changes (Fig. 6). In their northernmost part, these two subunits onlap on the truncated surface observed at the top of lithological unit 3, comprising the fenestral-microbial facies (Fig. 2). A few tens of metres south, the basal part of these two subunits displays centimetre-thick beds characterized by basal erosive surfaces (Fig. 5a, c). These thin beds consist of a grain-supported sediment particularly rich in large pisoids with some gastropods and ostracods (Figs 5c, d, 6a). Quartz grains are present to common, poorly to moderately sorted and subangular to subrounded. Several tens of metres south, the base of subunit 4b consists of sediments that have a mud-supported texture with only sparse fragments of echinoderms and bivalves (Figs 6a, 7a, i). Quartz grains are present to common, moderately sorted and well rounded, associated with some subangular centimetre-scale cherty clasts.

Subunits 4a and 4b display a lower part characterized by one (subunit 4a) or several (subunit 4b) beds onlapping on the truncated surface at the top of

https://doi.org/10.1017/S0016756813000988 Published online by Cambridge University Press

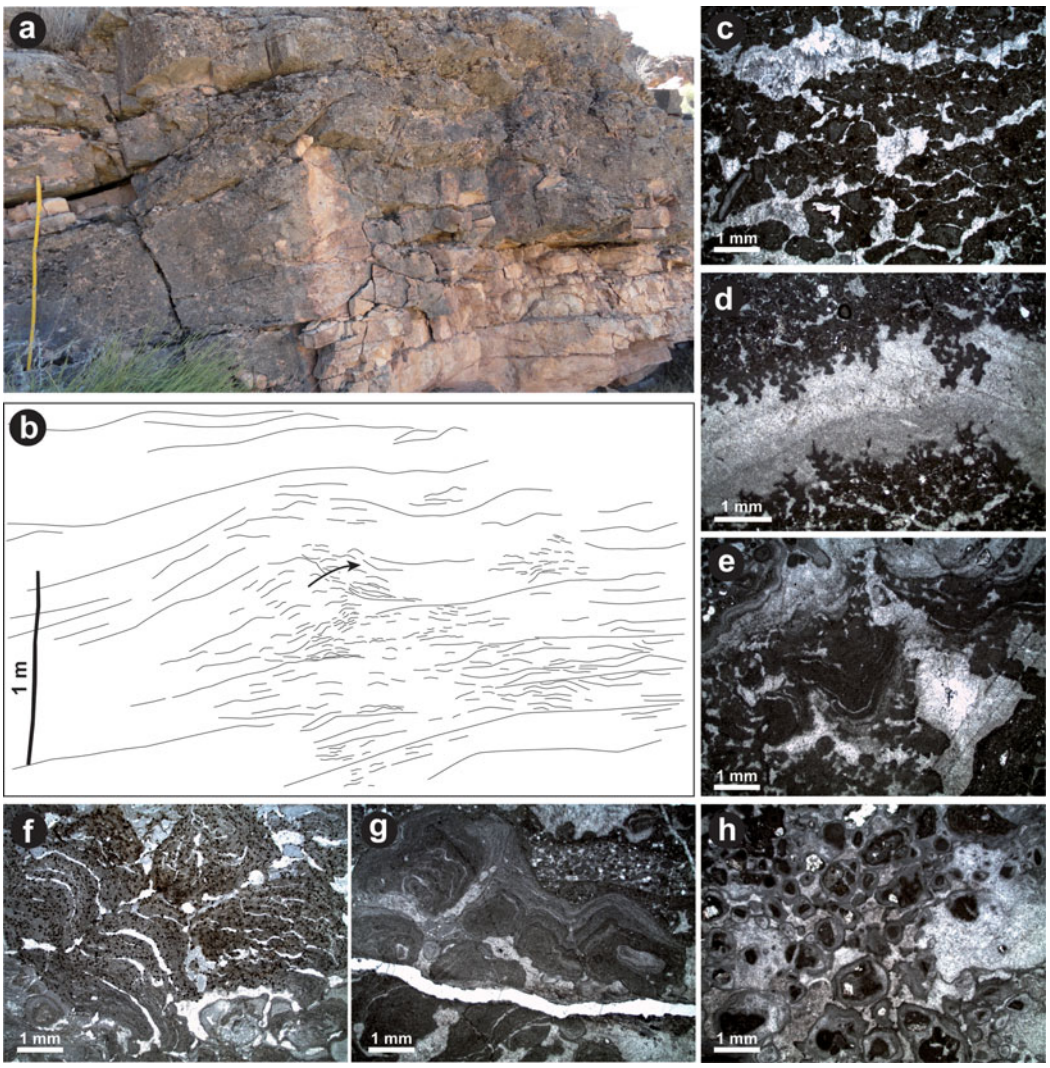

Figure 4. (Colour online) (a, b) Field view and sketch of the internal structure of fenestral-microbial limestone of lithological unit 3; note the lateral accretion inside metre-scale patch reefs (black arrow). (c–h) Various microfacies of this fenestral-microbial limestone. (c) Fenestral packstone with a framework made of abundant peloidal grains and some bivalve fragments. (d) Columnar microbial growth at the roof and at the floor of a large fenestral void. (e) Succession of sparry carbonate cements and micritic crusts in a large void area. (f) Domal micritic crusts with laminated sheets. (g) Pisoids with directional elongations; latest micritic laminae show interpisoid linkage. (h) Meniscus cements between pisoids.

lithological unit 3, comprising fenestral-microbial limestone facies (Fig. 2d, e). The onlapping bed of subunit 4a also shows lateral facies variations (Fig. 6). In a northern position, close to its onlap termination, the sediment displays a packstone (locally grainstone) texture and contains peloids, ooids (micritic and, to a lower extent, radial), undifferentiated bivalves, gastropods and echinoderm plates (Fig. 5e). Although preserved as incomplete internal moulds, numerous gastropods reach an unusually large size up to an estimated maximum of *c.* 9 cm (measured size *c.* 7 cm; Fig. 8). An ammonoid specimen (*Owenites* sp.) was observed associated with these gastropods. Beyond 50 m from the previous sampling zone, the sediment has a wackestone (locally packstone) texture with peloids, bivalves, serpulids, echinoderm plates and sparse micritic and radial ooids. In this lower part of subunit 4a, quartz grains are abundant, subrounded to subangular and moderately sorted.

The upper parts of subunits 4a and 4b display prograding sigmoids with downlap and toplap terminations (Fig. 2d, e). Sampled at the toe of the clinoform (*sensu* Quiquerez & Dromart, 2006), the sediments exhibit a packstone-wackestone texture with bivalves, gastropods, echinoderms, ostracods and sparse radial and micritic ooids (Fig. 5f). Quartz grains are common, subrounded and moderately sorted. Subangular pebbles of cherty extraclasts are present at the base of the clinobeds (Fig. 5a). Several tens of metres south of the toe of the clinoform, subunit 4b can be subdivided into two main beds that can be regarded as distal parts of a clinobed (Fig. 7a). These distal clinobeds show a net vertical facies evolution. In their lower part, sediments display a mud-supported texture with echinoderm plates, bivalves, ostracods and some lingulid brachiopods (Fig. 7a, h, f). Quartz grains are common to abundant, subangular to subrounded and relatively well sorted. The uppermost part of the beds shows a

https://doi.org/10.1017/S0016756813000988 Published online by Cambridge University Press

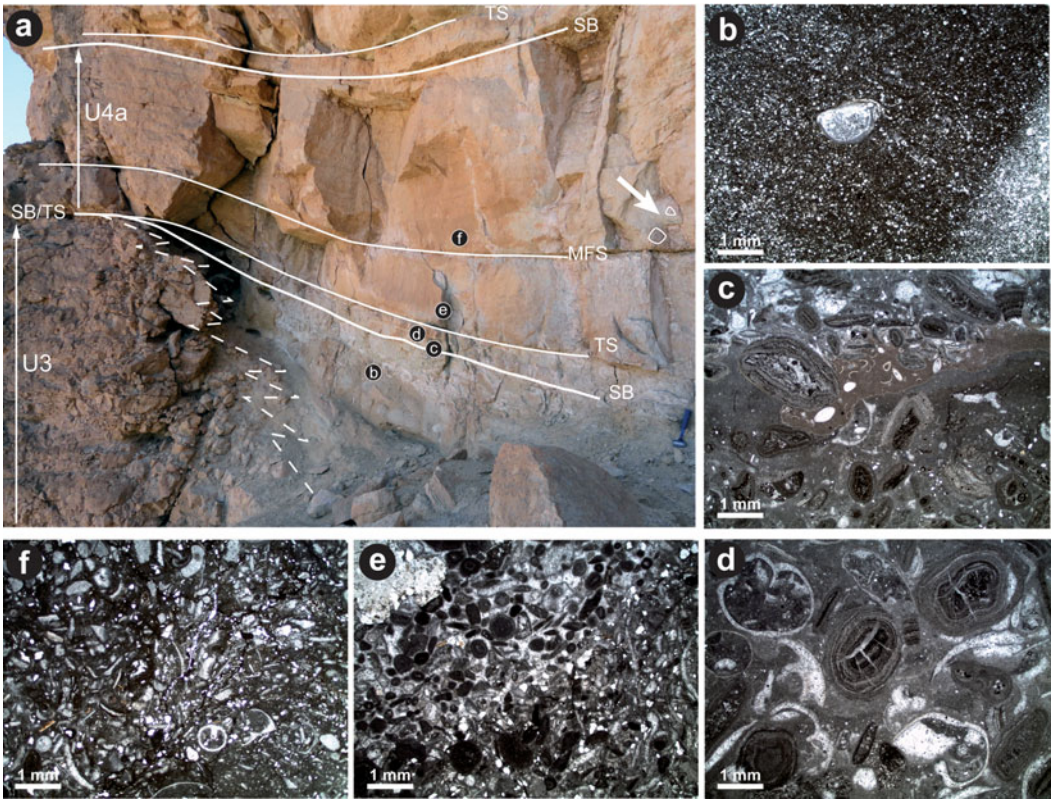

Figure 5. (Colour online) Field view illustrating (a) lateral facies variation (dashed line) between fenestral-microbial limestones and (b) dolomudstones in lithological unit 3 (U3); white arrow indicates angular extraclasts. (c) Erosional surface at the top of lithological unit 3; note ostracods just above this surface. (d) Cracked pisoids and gastropods. (e) Peloidal and bioclastic packstone (lower right corner) and a burrow infilled by a grainstone with peloids and ooids. (f) Bioclastic wackestone to packstone with gastropods, bivalves and echinoderms. U4 – lithological unit 4; SB – sequence boundary; TS – transgressive surface; MFS – maximum flooding surface.

grain-supported texture with gastropods, bivalves, echinoderm plates, ostracods, peloids and micritic and radial ooids (Fig. 7a, e, g). Quartz grains are abundant, subangular to subrounded and moderately sorted.

A few metres south of the toe of the clinoforms, both subunits are characterized by a dense and deep bioturbation marked by overabundant vertical trace fossils (Fig. 9). The entire bed thickness displays vertical or slightly oblique burrows that are circular in cross-section (Fig. 9a). Burrow diameters are between 0.5 and 2 cm. Burrow depth can reach up to 25 cm. Even if not always well preserved, these burrows show a U-shape apparently with no spreiten in between (Fig. 9b). Although a firm ichnogeneric assignment is difficult on the studied outcrop, these vertical burrows probably belong to the ichnogenus *Arenicolites* (R. Hofmann, pers. comm. 2013). Occasionally, some horizontal burrows (apparently not branching) are observed in these beds. Since outcrop conditions did not allow us to investigate their lining and sedimentary infill, these burrows belong either to the ichnogenus *Palaeophycus* or to *Planolites* (R. Hofmann, pers. comm. 2013).

3.e. Lithological unit 5

Lithological unit 5 exhibits a vertical facies evolution (Fig. 7). Sediments of the thin (*c.* 30 cm thick) basal part are represented by a packstone (locally wackestone) texture with abundant and coarse fragments of echinoderms, bivalves and serpulids (Fig. 7a, d). This basal interval is strongly bioturbated and contains abundant, moderately well sorted and subrounded quartz grains. Notably, it also contains small isolated spheroid siliceous sponges that do not exceed *c.* 1 cm in diameter. These isolated sponges resemble lyssacine hexactinellids previously described from ramp environments in the Smithian of central Utah and Spathian of Nevada (Brayard *et al.* 2011*b*). The lower part of lithological unit 5 consists of a thick interval of wackestone with peloids and sparse echinoderm plates. Quartz grains are very abundant, well sorted and subrounded. This interval is still densely bioturbated and shows low-angle cross-stratification. The upper part of lithological unit 5 consists of a bioturbated and bioclastic grainstone (locally packstone) with abundant bivalves, gastropods and peloids. Some fenestrae are visible within peloidal horizons. Quartz grains are common to abundant, well sorted and subangular. This facies is characterized by angular cross-stratifications and herringbone cross-bedding structures with high amalgamation.

3.f. Lithological unit 6

Lithological unit 6 corresponds to a metre-scale interval that generally forms the top of the studied cliff (Fig. 2).

https://doi.org/10.1017/S0016756813000988 Published online by Cambridge University Press

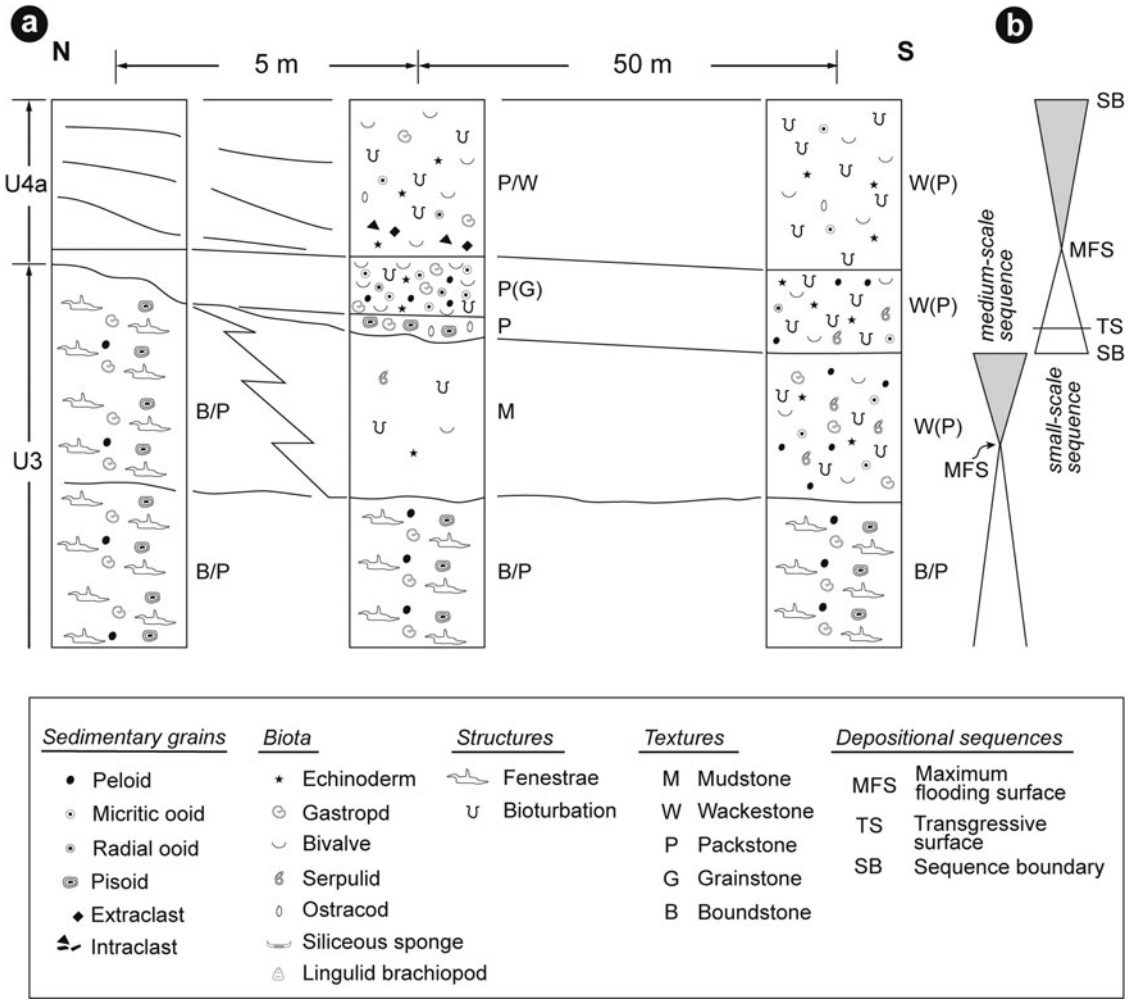

Figure 6. (a) Vertical and lateral facies variations at transition between lithological units 3 and 4. Not to scale. (b) Sequential interpretation.

Along a N–S transect, this unit shows a marked lateral facies variation (Fig. 10). In the northernmost part of the outcrop, sediments display a wackestone (locally packstone) texture with common bivalves and gastropods, and some serpulids. There are also common micritic ooids, some cortoids and possible *Favreina* (Fig. 10b). Quartz grains are not observed. A second facies type rests vertically directly on the discontinuity observed at the top of the thickest interval of lithological unit 3, which constitutes a topographic high. This facies displays a grainstone texture with abundant recrystallized bivalves, gastropods and rare ostracods (Fig. 10c). Abundant peloids and micritic ooids are also present. No detrital quartz was observed. South of the topographic high, the sediments exhibit a packstone (locally wackestone) texture with abundant bivalves and gastropods (Fig. 10d). Echinoderm plates and serpulids represent additional fauna. Micritic ooids and peloids are also common. Quartz grains are present, rounded and well sorted. In the southernmost part of the study area, the sediment displays a packstone texture with abundant thin-shelled bivalves, some serpulids and echinoderm plates. These bivalves can be vertically oriented or show umbrella structures. In this later case, the valves shield underlying siliceous sponges (Fig. 10e). Quartz grains are rare and rounded.

3.g. Lithological unit 7

Lithological unit 7 sets back from the cliff and can be observed only along local low-relief outcrop surfaces (Fig. 2a). Its facies corresponds to a bioclastic grainstone (locally packstone) with abundant bivalves, some ooids and peloids and possibly some *Favreina*. Locally, some fenestrae, mud clasts and mud draps are also observed. Quartz grains are common to abundant, well sorted and subrounded.

4. Depositional models

The progressive gradation between deposits of lithological units 2 to 3 is consistent with a first single depositional model (Fig. 11a). Previous studies interpreted the Rock Canyon Conglomerate (i.e. lithological unit 2) as palaeochannel deposits and thin regolithic breccias (Lucas, Krainer & Milner, 2007). Nielson (1991) considered that coarse to fine cross-bedded clastic rocks suggest deposition as a fan delta. Our observations reveal a lower breccia subunit with

https://doi.org/10.1017/S0016756813000988 Published online by Cambridge University Press

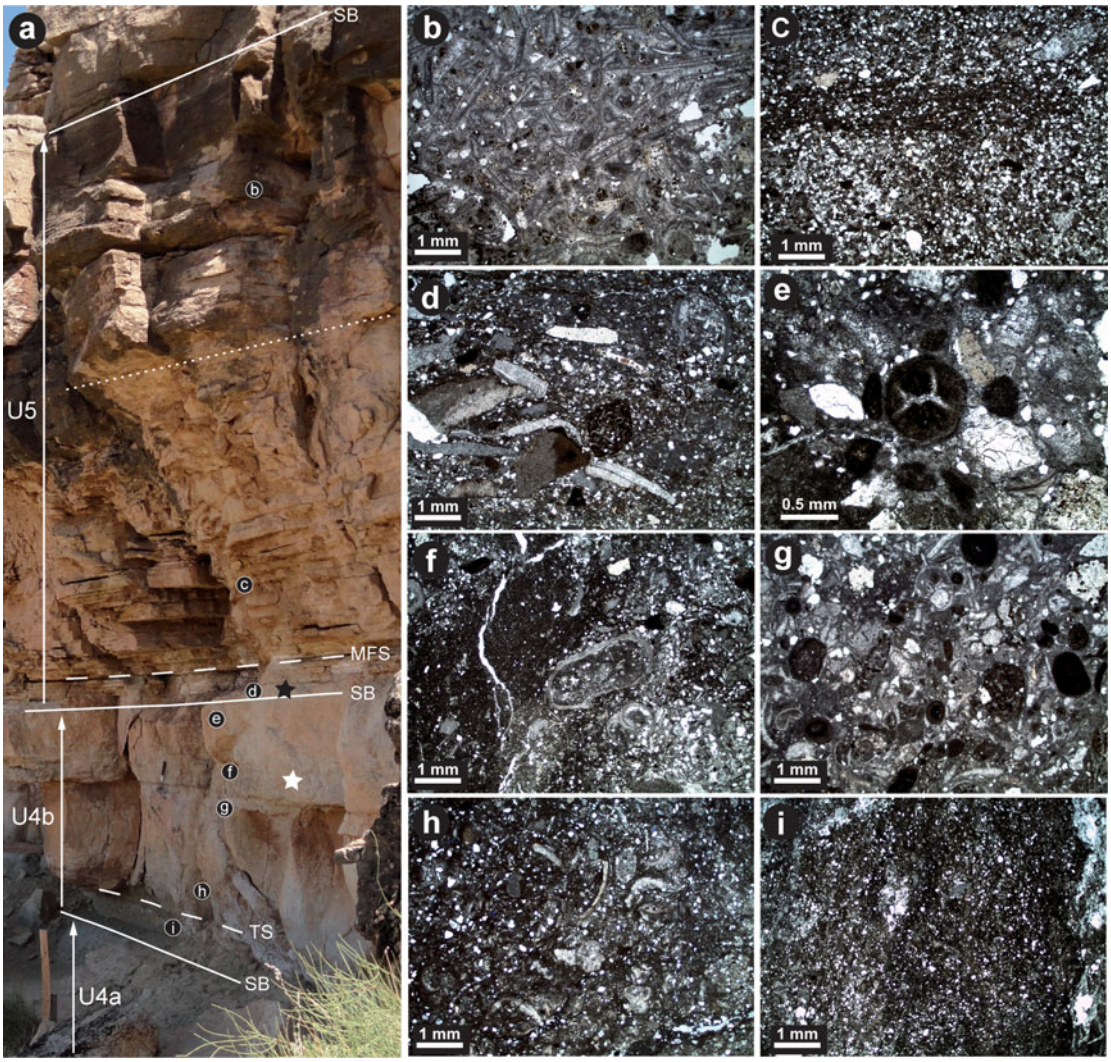

Figure 7. (Colour online) (a) Field and (b–i) microfacies illustrations of lithological units 4b and 5. (a) Lingulid brachiopods (white star) are present in subunit 4b, and small rounded siliceous sponges (black star) are present at the base of lithological unit 5. (b) Grainstone (locally packstone) consisting of abundant recrystallized bivalves, some echinoderms, gastropods, peloids and detrital quartz. (c) Dolomitized wackestone rich in quartz, with sparse echinoderm fragments. Dotted line in lithological unit 5 separates the two main subunits illustrated in (b) and (c). (d) Wackestone (locally packstone) composed of abundant echinoderms, bivalves and rare serpulids; quartz is abundant. (e) Packstone (locally wackestone) consisting of echinoderms, bivalves, gastropods, peloids and ooids; quartz is present. Note the shrinked structure of micritic ooids. (f) Wackestone composed of abundant echinoderms, bivalves, gastropods and rare serpulids; quartz grains are relatively large and abundant. (g) Packstone consisting of abundant peloids, echinoderms, gastropods, bivalves, serpulids and radial (and micritic) ooids; quartz is abundant. (h) Wackestone composed of echinoderms and bivalves; quartz is common. (i) Dolomitized mudstone-wackestone with sparse fragments of echinoderms and bivalves. Legend as in Figure 6.

sandy matrix-supported clasts that lack imbrication and internal stratification (Fig. 3a), pointing to debris flows in an alluvial context. Even if a marked Permian palaeorelief was not observed in the studied area, the palaeogeographical reconstruction of Blakey (1979) indicates a chert-pebble alluvial plain west of Hurricane at the front of low hills consisting of cherty Kaibab Formation in the area of the present Virgin Anticline. The second subunit of lithological unit 2 reveals conglomerates with planar cross-bedded gravels (Fig. 3b), which can reflect lateral out-building from longitudinal bars. This conglomeratic subunit is overlain by silty to muddy deposits of a third subunit (Fig. 3c). These later deposits suggest migration of active to inactive tracts.

The succession of the three subunits observed in lithological unit 2 (i.e. breccia, conglomerates and silts) therefore reflects an evolution from an alluvial fan to more distal rivers and flood plains. The transition to a tidal flat is progressively recorded at the base of lithological unit 3 where fenestral-microbial carbonates still contain abundant cherty clasts (limestone conglomerate of Blakey, 1979; Fig. 3d). Lithological unit 3 is characterized by a lateral facies zonation from peritidal to shallow subtidal settings (Fig. 11a). Peritidal carbonates (*sensu* Flügel, 2004), that is, shallow-subtidal, intertidal and supratidal sediments formed in marginal-marine and shoreline depositional environments, correspond to the fenestral-microbial facies. The association of stromatolites, fenestral pores and *in situ* brecciation are consistent with frequently exposed parts of tidal flats (Flügel, 2004). The observed fauna (i.e. sparse ostracods, gastropods and bivalves) is also

https://doi.org/10.1017/S0016756813000988 Published online by Cambridge University Press

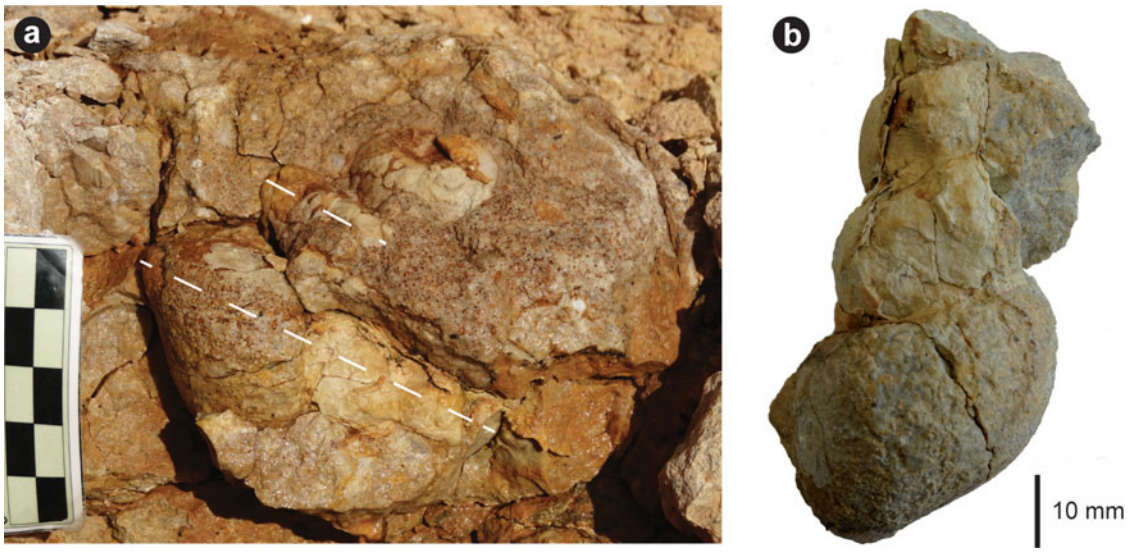

Figure 8. (Colour online) (a) Field illustration of Smithian large-sized gastropod specimens from Timpoweap Canyon, lithological unit 4a. (b) Close-up of a single specimen. Dashed lines indicate shell-coiling axis. Specimen number: Université de Bourgogne Géologie Dijon, UBGD 275164.

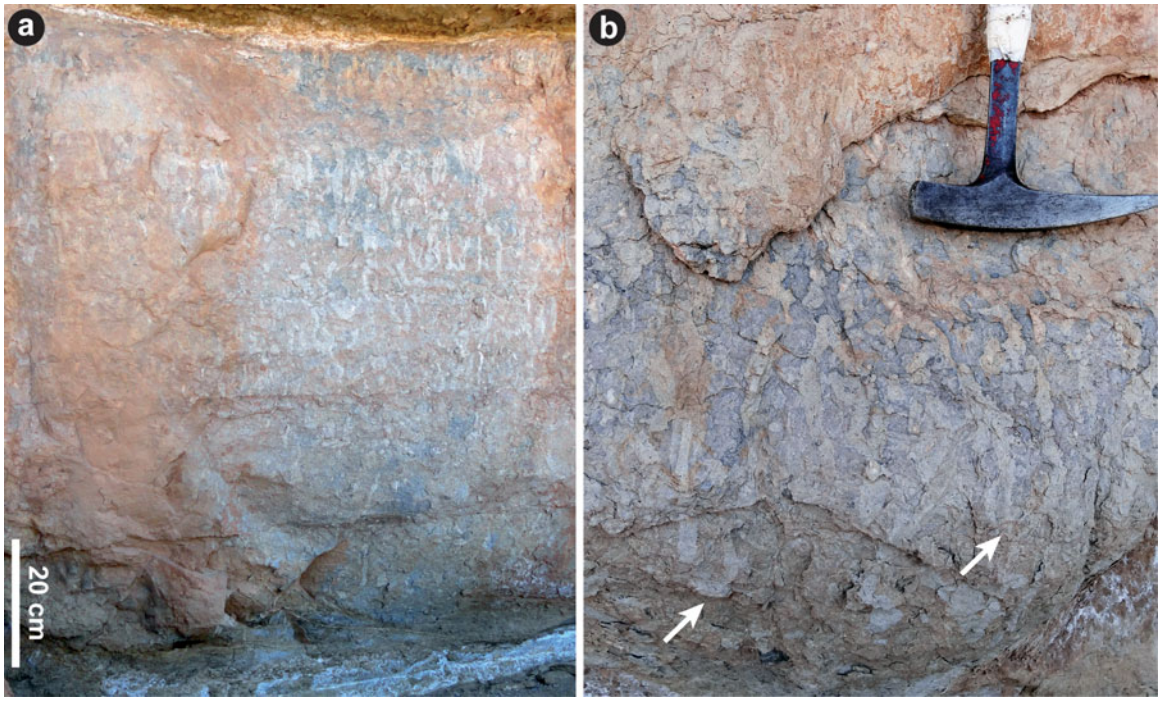

Figure 9. (Colour online) Field observations of the intense bioturbation in lithological unit 4. (a) Basal and lower parts of subunit 4a; burrows are present in the entire bed thickness. Note the minor surfaces inside the bed that mark the successive phases of colonization by bottom dwellers. (b) Lower part of subunit 4b; note that burrows are up to 25 cm in depth and display a basal U-bend from pair association (white arrows, hammer for scale).

consistent with an intertidal environment (Flügel, 2004). Pisoids and meniscus cement suggest vadose-marine environments in supratidal areas (Esteban and Pray, 1983; Peryt, 1983). Lateral accretion and minor truncation surfaces observed in low-relief patch-reef structures indicate reduced accommodation and recurrent erosional phases (Figs 2, 4a, b). Bioturbated dolomudstones with rare organisms (i.e. serpulids, bivalves and echinoderms) observed laterally to the fenestral-microbial facies (Figs 5, 6) reflect a more important available space for sedimentation in a shallow subtidal marine setting (Fig. 11a). At a more distal position (a few tens of metres to the south), the sediments become more bioclastics with gastropods, serpulids, bivalves and echinoderms. Even though few ooids are observed, the mud-supported texture still implies a low-energy setting protected from the open ocean. Such protection can result from the existence of a wide epeiric platform dampening incoming waves, positioned behind a barrier or within a restricted embayment. The presence of equivalent deposits (i.e. Sinbad and Timpoweap formations) between the eastern and western

https://doi.org/10.1017/S0016756813000988 Published online by Cambridge University Press

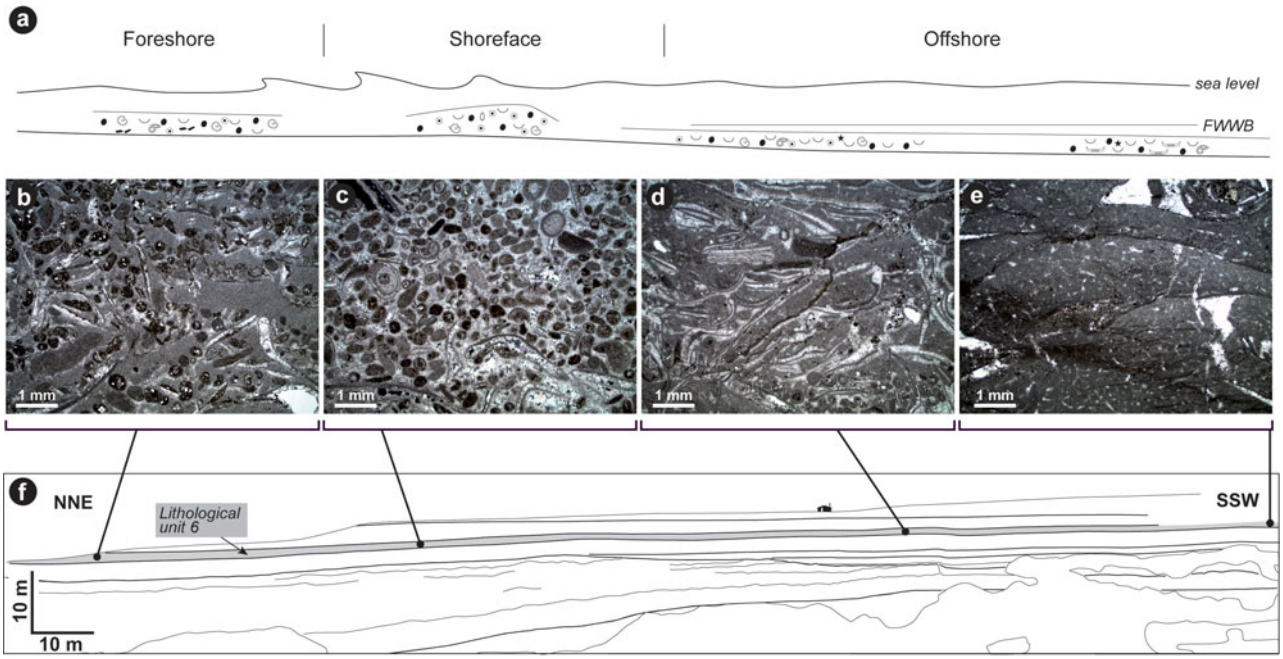

Figure 10. (Colour online) (a) Depositional model for lithological unit 6. (b–e) Microfacies illustrations along a N–S transect in Timpoweap Canyon as illustrated in (f). (b) Wackestone with common bivalves and gastropods, some serpulids, common micritic ooids, some cortoids and possible *Favreina*. (c) Grainstone with abundant recrystallized bivalves, gastropods, rare ostracods, abundant peloids and micritic ooids. (d) Packstone with abundant bivalves and gastropods, common micritic ooids and peloids. (e) Packstone with abundant thin bivalves. Note that these bivalves show umbrella structures and that the pelecypod valves shielded underlying siliceous sponges. FWWB – fair-weather wave base. Legend as in Figure 6.

parts of southern Utah (Blakey, 1979; Lucas, Krainer & Milner, 2007) suggests an embayment that opened to the north to a larger epicontinental basin (Brayard *et al.* 2013). This first facies model deduced from lithological units 2 and 3 highlights a fluvial-marine transitional environment from a coastal plain (see also Blakey, 1979) to an embayment system.

The analysis of the two subunits of lithological unit 4 indicates a significant change in topography that strongly modified the depositional settings (Fig. 11b). Attached to an antecedent topography that resulted from truncation of the fenestral-microbial limestones (lithological unit 3), subunits 4a and 4b can be assimilated to clinothems that are made of clinobeds bound by hiatal surfaces (Fig. 2d, e). If the flat-topped upper and middle slope parts of the clinoforms could not be sampled, the toe-of-slope part of the first clinothem (i.e. subunit 4a) consists locally of grain-supported sediments (Figs 5f, 6a). These latter sediments are also strongly bioturbated and composed of bivalves, gastropods, peloids, ooids and echinoderms. Such facies suggests deposition in an open marine setting at the transition between nearshore and offshore settings (Fig. 11b). The presence of large limestone gravels in the lower part of subunit 4a indicates that erosion was still active at the top of the underlying fenestral-microbial limestones of lithological unit 3 (Fig. 5a). Sampled in a more distal position (Fig. 7), sediments of the second clinothem (i.e. subunit 4b) display a mud-supported fabric with bivalves, echinoderms, sparse ostracods and rare ooids. The observed ichnoassemblage, with a high density of putative *Palaeophycus* or *Planolites*, reflects an intense colonization by bottom dwellers between storm periods. Subunits 4a and 4b correspond to metre-scale clinoforms that are characterized by rapid lateral facies changes over a few tens of metres. Such a pattern suggests a shallow proximal setting above fair-weather wave base (Quiquerez & Dromart, 2006). In these clinothems grain-supported sediments have a limited extension (i.e. a few tens of metres close to the shoreline position), suggesting a low-wave-energy embayment system.

Lithological unit 6 was sampled laterally (Fig. 10). Lateral facies distribution suggests that the inherited topography may have still influenced the sedimentation under a wave-dominated regime. Observed where lithological unit 3 is the thickest, the deposition of an oolitic grainstone suggests a shoreface setting (Fig. 11c). Protected behind these high-energy deposits, mud-supported sediments may have been deposited. Below the fair-weather wave base, offshore deposits correspond to a bivalve-rich packstone. Some of these bivalves shielded underlying siliceous sponges (Fig. 10e) whereas others are vertically oriented, suggesting local turbulent and rotary flows during storms (Pérez-López & Pérez-Valera, 2011). This third depositional model suggests a marginal area where sedimentation was either tide or wave dominated.

Facies observed in lithological units 5 and 7 likely reflect more internal peritidal settings compared to deposits of lithological unit 6 (Fig. 11d). Angular cross-stratification, herringbone cross-bedding and local peloidal horizons observed in the upper part of lithological unit 5 indicate a tide-dominant regime. The

https://doi.org/10.1017/S0016756813000988 Published online by Cambridge University Press

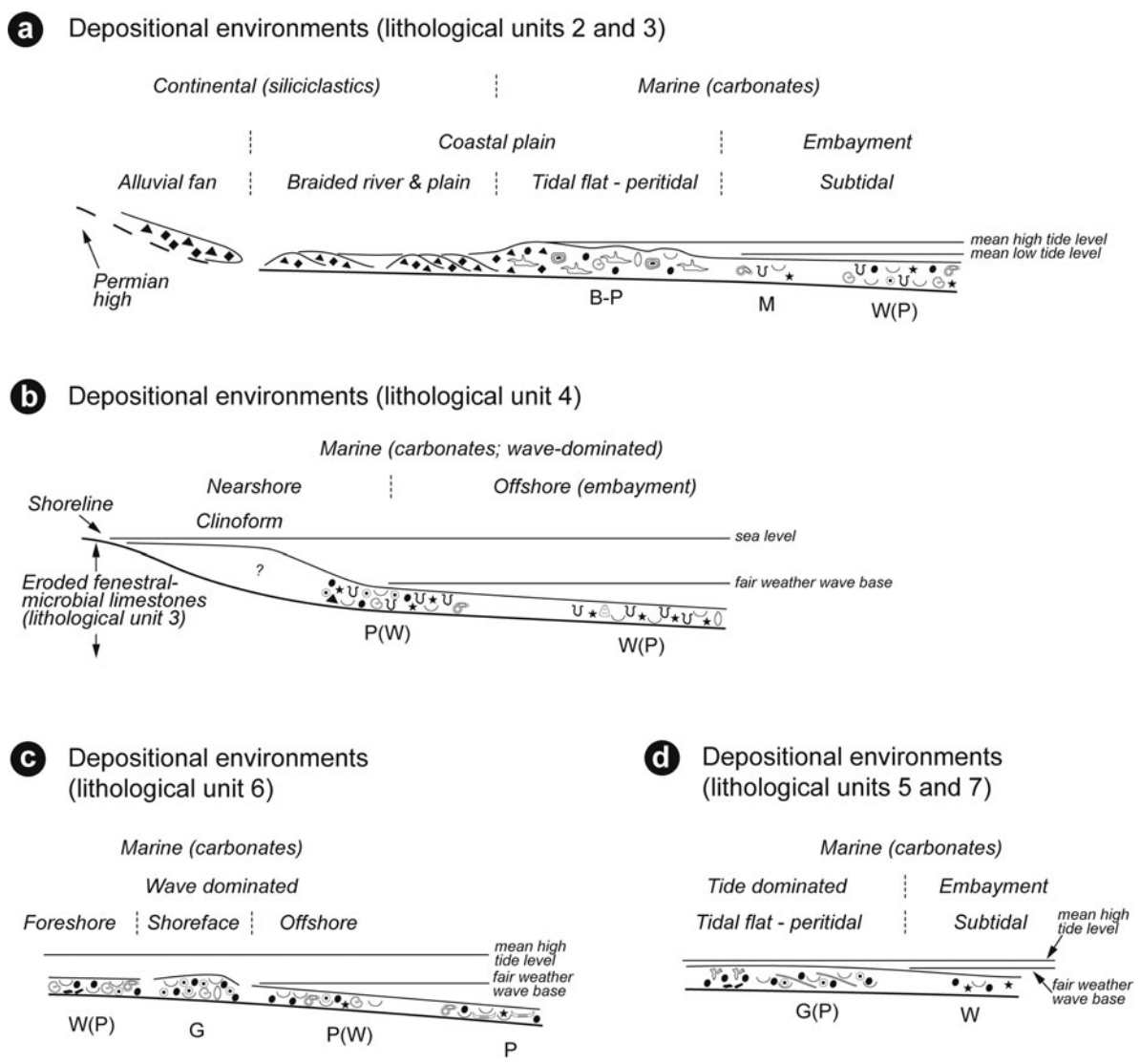

Figure 11. Depositional models deduced from the Timpoweap sedimentary succession. Depositional environments for: (a) lithological units 2 and 3; (b) lithological subunits 4a and 4b; (c) lithological unit 6; and (d) lithological units 5–7. Legend as in Figure 6.

presence of fenestrae and mud intraclasts may reflect more internal tidal flats. The lower part of lithological unit 5 consists of mud-supported bioclastic sediments rich in echinoderms and quartz (Fig. 7a, c), suggesting deposition in a marine offshore setting of a low-energy embayment system.

5. Transgressive-regressive cycles and shoreline migrations

Stratal stacking patterns and surface geometries observed in Timpoweap Canyon reveal at least three different orders of transgressive-regressive sequences (Fig. 1b). Above the Rock Canyon Conglomerate, the lithological succession can be replaced by a long-term transgressive trend. Inside this transgressive trend, lithological units 2 and 3 illustrate a complete first medium-scale sequence that ends at the erosional truncation surface (Fig. 2). Lithological units 4–7 record the transgressive interval of a second depositional sequence. The regressive interval of this sequence probably corresponds to deposits of the Lower Red Formation. This latter formation overlies the Sinbad Formation (Blakey, 1979; Lucas, Krainer & Milner, 2007). Four additional small-scale sequences are also well visible within lithological units 4–7 (Figs 1, 12).

Deposition of fenestral-microbial limestones (i.e. lithological unit 3) reflects a progressive marine incursion on a chert pebble alluvial plain (Blakey, 1979). Transgression of the Early Triassic sea within central and southern Utah – probably during the early Smithian in this area (Brayard *et al.* 2013) – resulted in deposition of the limestones of the Sinbad Formation (Nielson, 1991). This first long- and medium-scale transgressive interval is highlighted by a retrogradational stacking pattern of deposits in the lower part of lithological unit 3 (stage 1, Fig. 12). Microbial patchy morphologies have larger dimensions in the middle part of this unit, suggesting higher accommodation and thus an interval of maximum flooding for the first identified medium-scale transgressive-regressive depositional sequence (Fig. 1b). Stratal terminations in the uppermost

https://doi.org/10.1017/S0016756813000988 Published online by Cambridge University Press

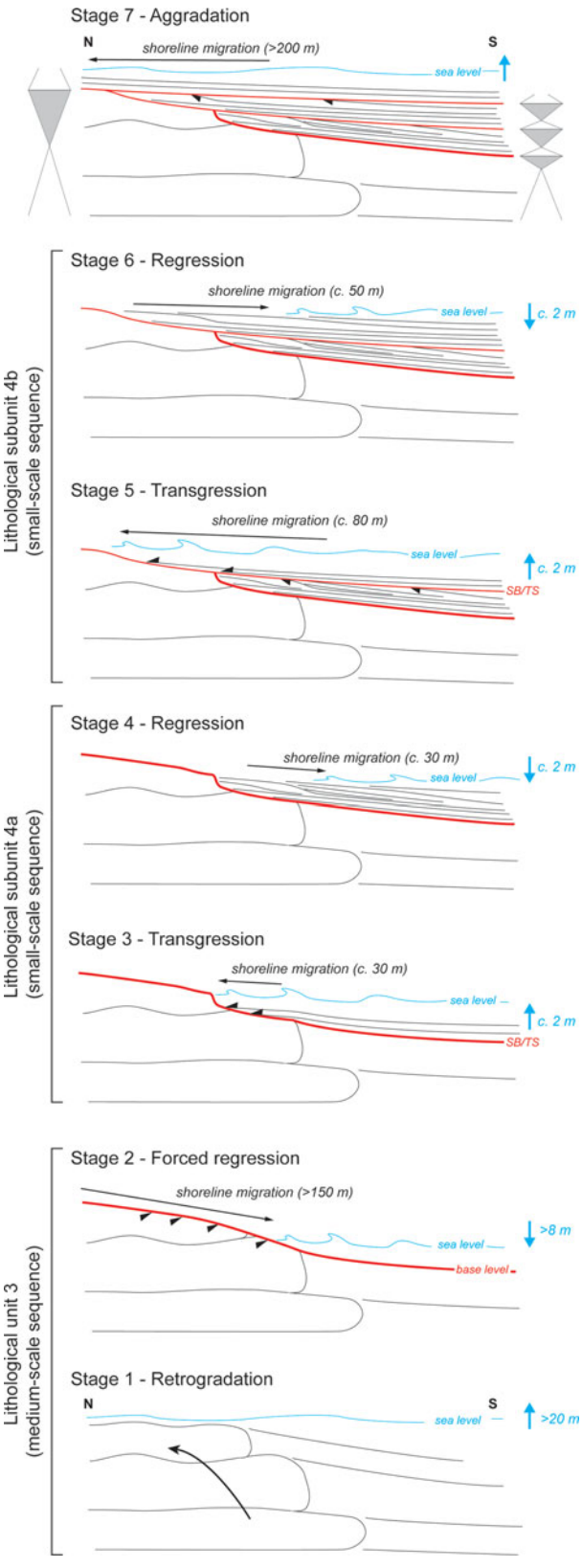

Figure 12. (Colour online) Reconstruction of Early Triassic medium-scale (lithological unit 3) and small-scale (lithological subunits 4a and 4b) sequences, and successive stage of shoreline migrations along the sedimentary succession observed in Timpoweap Canyon.

part of fenestral-microbial unit 3 correspond to a truncation that implies a net accommodation loss associated with an erosional phase. Such an erosional surface reflects a forced regressive trend (stage 2, Fig. 12). The peritidal setting of fenestral-microbial deposits coupled with relative sea-level changes could have preferentially caused an emersion and erosion up to the formation of a local palaeorelief that gradually dipped to the south (Fig. 2a, b). The shoreline migration probably exceeded 150 m southwards, that is, the lateral extent of the outcrop where truncation is visible at the top of lithological unit 3. Lateral to this fenestral-microbial facies, dolomudstones are progressively enriched in pisoids and finally exhibit an uneven erosional surface in their stratigraphic uppermost part. As toplap terminations are no longer observed, this erosional surface probably reflects wave scouring in a shallow marine setting during the later stages of base level fall. This erosional surface is interpreted as the sequence boundary of the first identified medium-scale transgressive-regressive sequence (Figs 1b, 5a, c, 6).

A thin double bed formed of pisoids with abundant shrinkage structures overlies this surface (Fig. 5d, e). These pisoids were probably removed from subaerial unconformity at the top of lithological unit 3 and redeposited in a shallow subtidal setting. Considering a negligible compaction for deposits of lithological unit 3 – absence of stylolites coupled with a rapid lithification of microbial deposits – this forced regressive trend resulted in a sea-level fall of more than 8 m. This estimate corresponds to the thickness of fenestral-microbial limestone unit 3 that exhibits the truncation.

A first small-scale transgressive-regressive sequence is recorded within lithological subunit 4a. The transgressive interval corresponds to successive beds that onlapped against the truncated surface at the top of lithological unit 3 (Figs 2d, 5a, c). A putative berm crest may reflect the shoreline position at the end of the transgression (Fig. 2d). In that case, the shoreline migration accompanying this transgressive trend can be estimated to be *c.* 30 m northwards (stage 3, Fig. 12). The corresponding relative sea-level rise is estimated to be *c.* 2 m. Successive clinoforms mark a normal regressive trend of this first small-scale sequence (stage 4, Fig. 12). The latter erosional transgressive surface makes it difficult to estimate the position of the shoreline at the end of the regression. Shoreline position should not exceed the more distal truncated clinobed, which probably reflects wave scouring in a shallow marine setting during the later stages of a base level fall. In that case, the shift in shoreline during this regressive trend was probably close to 30 m southwards, and the corresponding sea-level fall was close to 2 m.

The second small-scale sequence corresponds to subunit 4b. The basal part of this subunit displays successive beds that onlapped against the erosional transgressive surface at the top of lithological unit 4a (stage 5, Fig. 12). A new putative berm crest marks the shoreline position at the end of the transgression (Fig. 2e). The shoreline position shifted about 80 m northwards and the corresponding sea-level rise did not exceed *c.* 2 m. Similar to the previous small-scale sequence, successive clinoforms indicate a regression.

https://doi.org/10.1017/S0016756813000988 Published online by Cambridge University Press

The southernmost eroded clinobed observed in the uppermost part of subunit 4b suggests a shoreline migration of <50 m and a sea-level fall of <2 m (stage 6, Fig. 12).

With vertical stacking patterns, lithological units 5–7 do not allow us to further reconstruct shoreline trajectories (Fig. 2). However, this sedimentary succession suggests two additional small-scale sequences of relative sea-level changes. The first (i.e. third small-scale sequence; Fig. 1b) is recorded in lithological unit 5. At the base of the unit, a multi-centimetre-thick interval of limestones, rich in coarse echinoderm fragments and sparse siliceous sponges, was deposited during a relative sea-level rise (Fig. 7a). The corresponding transgressive trend was marked by a shoreline migration that exceeded 200 m – i.e. the lateral extent of the outcrop where lithological unit 5 is visible over lithological unit 3 (stage 7, Fig. 12). A thin marly horizon probably reflects the maximum flooding interval. A dolomicrite limestone with sparse echinoderms and overlying tidal bivalve-rich grainstones may indicate a relative sea-level fall (Figs 7a, 11d). The last small-scale sequence includes deposits of lithological units 6 and 7. Wave-dominated bivalve-rich limestones of lithological unit 6 were deposited during a relative sea-level rise, whereas deposition of tide-dominated bivalve-rich limestones reflects a relative sea-level fall.

The erosional phase leading to truncation at the top of lithological unit 3 triggered an increment of accommodation over a few tens of metres along a N–S proximal-distal axis (Fig. 2). Two small-scale sequences with successive clinoforms are observed at a southern (i.e. distal) position, whereas these are absent from a proximal position (Fig. 12). During the transgressive trend at the base of lithological unit 5 the antecedent relief was largely filled by deposits of lithological unit 4, leading to a shoreline migration exceeding several hundreds of metres (stage 7, Fig. 12). Sampling difficulties did not allow us to highlight the influence of palaeotopography during deposition of lithological unit 5. Nevertheless, inherited topography still influenced the sedimentation of lithological unit 6, as suggested by deposition of oolitic grainstones on a residual topographic high (Fig. 10). The Timpoweap sedimentary succession therefore reflects peritidal to shallow subtidal settings, which were adequate to record rapid shoreline migrations. In such a context topographic highs of restricted local extent can be formed, leading to the recording of a different number of depositional sequences according to the position along the coastline (Fig. 12). A complex and irregular coastline is also suggested during the Smithian when comparing the northwards polarity of the observed depositional system with the global trend of the Early Triassic transgression at a regional scale. Indeed, the Smithian advancement of the sea seems to have proceeded southwards along a corridor within Utah (Collinson, Kendal & Marcantel, 1976; Nielson, 1991; Paull & Paull, 1993; Dickinson, 2006; Brayard *et al.* 2013). Moreover, the enlarged palaeogeographical reconstruction of the studied area by Blakey (1979) indicates another general polarity of the depositional system, with topographical highs located on the west and an open sea on the east. The observed sedimentary succession in Timpoweap Canyon suggests that, at least locally, the continental to marine open depositional system can display a N–S polarity.

6. Relative sea-level changes

Global sea-level curves generally rise across the Permian–Triassic boundary (Haq & Al-Qahtani, 2005; Haq & Shutter, 2008; ICS, unpub. data, 2011: http://www.stratigraphy.org). In this global trend, Early Triassic sea-level changes of higher frequency are not easily dated and correlated, which explains why they are rarely considered (Embry, 1997). Lehrmann *et al.* (2007) identify several third-order sea-level sequences in the Beisi Formation of the Chongzuo–Pingguo platform (South China). In SW Utah, the Lower Triassic sedimentary succession recorded three third-order transgressive-regressive sequences that originated in the Griesbachian, Smithian and earliest middle Spathian (Embry, 1997; Paull & Paull, 1997). Deposition of the Rock Canyon Conglomerate could have followed the tectonic uplift linked to the Sonoma Orogeny (Collinson, Kendal & Marcantel, 1976; Nielson, 1991; Dickinson, 2006). The lack of biostratigraphic markers makes it difficult to assign a more precise age, which was dated as either Permian or Early Triassic (Gregory, 1950; Reeside & Bassler, 1922; Blakey, 1979). In Timpoweap Canyon, the gradual transition between continental and marine deposits corresponds to the transition between the Rock Canyon Conglomerate and limestones of the Sinbad Formation that was considered as middle–late Smithian in age (Brayard *et al.* 2013). The presence of O*wenites* sp. in the deposits just above the fenestral-microbial lithological unit 3 allows us to specify a middle Smithian age for the Sinbad Formation. This sedimentary evolution can be placed into the third-order Smithian sea-level rise identified by Embry (1997).

The identification of medium- and small-scale depositional sequences in the Sinbad Formation reflects high-frequency relative sea-level fluctuations. Small-scale depositional sequences observed in lithological units 4–7 are of middle–late Smithian age, representing a total maximum duration of <400 ka (see estimates by Brühwiler *et al.* 2010). If high-frequency (i.e. Milankovitch and sub-Milankovitch) cycles appear to have been recorded in Lower Triassic sedimentary successions (e.g. Huang *et al.* 2011; Wu *et al.* 2012), corresponding sea-level changes were only suspected (Lucas, Krainer & Milner, 2007; Chen, Fraiser & Bolton, 2012). Observed small-scale depositional sequences are asymmetrical with thin transgressive deposits and thicker regressive deposits. Such an asymmetrical pattern of sequences is typical of short-term sea-level variations that are induced by glaciation–deglaciation cycles (e.g. Shackleton, 1987; Ruddiman,

https://doi.org/10.1017/S0016756813000988 Published online by Cambridge University Press

2003; Ridente *et al.* 2012). However, the amplitude of sea-level fluctuations indicated by the small-scale depositional sequences of lithological units 4–7 does not exceed *c.* 2 m. Such low-amplitude sea-level change is consistent with the absence of evidence for continental glaciation during Early Triassic time (Frakes, Francis & Syktus, 1992; Sano *et al.* 2012). In that case, these high-frequency sea-level changes may be interpreted to be the result of intense thermal expansions of the world ocean triggered by global warming (e.g. Kidder & Worsley, 2004). Particularly warm seawater temperatures during the middle–late Smithian (cf. Romano *et al.* 2013) support such an explanation. Alternatively, a sudden drop in sea level of at least 8 m triggered the formation of a palaeorelief at the top of lithological unit 3. Such a sea-level drop could have a tectonic origin related to the Sonoma Orogeny, which is responsible for regional uplift during the transition from Permian to Triassic (Collinson, Kendal & Marcantel, 1976). Thus, large- and medium-scale depositional sequences identified in the Timpoweap Canyon succession are consistent with regional uplifts, whereas small-scale depositional sequences may have been climatically driven.

7. Depositional settings and regional biotic recovery

Within Timpoweap Canyon, the oldest Triassic fossils are documented from lithological unit 3. This unit shows important lateral facies variations with fenestral-microbial limestones in peritidal settings and dolomudstones and bioclastic limestones in shallow marine subtidal settings (Fig. 11a). In the fenestral-microbial limestones, benthic organisms (gastropods, bivalves, ostracods and rare putative siliceous sponges) are poorly diversified. Microbial deposits are responsible for the edification of small patches that do not exceed a few metres in thickness (Figs 2, 4). Associated with rare putative siliceous sponges, these patches do not have a complex framework made of skeletal metazoans as was observed in other Smithian or Spathian reefs from Utah (Brayard *et al.* 2011*b*; Marenco *et al.* 2012). Patches observed in Timpoweap Canyon therefore cannot be considered as true metazoan-microbial reefs. This also suggests that Lower Triassic microbial-dominated limestone units (i.e. basal limestones of the Sinbad Formation) can show important differences in terms of biotic associations and frameworks at the scale of the western USA basin.

The benthic assemblage observed here in association with microbial deposits is well known worldwide in the aftermath of the end-Permian mass extinction (Sano & Nakashima, 1997; Kershaw *et al.* 2007, 2012). These metazoans are classically interpreted as representing low-diversity communities whose structure reflects harsh environmental conditions (Yang *et al.* 2011; Forel *et al.* 2013). They are typically composed of opportunistic or disaster forms dwelling in microbial ecosystems. However, in Timpoweap Canyon, the peritidal fenestral-microbial limestones are observed laterally to shallow bioclastic and bioturbated limestones with echinoderms, gastropods, serpulids and bivalves. Such a relatively diversified fauna suggests subtidal and marine conditions. It also seems to indicate that the biotic recovery was well underway contemporaneously with deposition of the fenestral-microbial limestones, at least locally. This observation questions the putative anachronistic and disaster character commonly attributed to microbialites in the western USA basin (Schubert & Bottjer, 1992; Pruss & Bottjer 2004; Pruss *et al.* 2006; Baud, Richoz & Pruss, 2007; Woods, 2009, 2013). Another example of a massive microbial mound that laterally passes to bioclastic packstones deposited in normal marine conditions was recently illustrated in the upper Anisian of Iran (Berra *et al.* 2012). Thus, the presence of microbial deposits in western USA does not necessarily indicate widespread harsh marine conditions. Rather, it underlines the preponderant role of the depositional environment upon the facies and biota distribution along a complex regional Early Triassic coastline.

In lithological unit 4, depositional settings evolved to a wave-dominated ramp system implanted on an inherited topography (Fig. 11b). In this facies model, microbial deposits are no longer observed. The absence of a large peritidal area coupled with relative high-energy conditions in an inner ramp setting probably did not allow the installation and stabilization of biofilms. The faunal assemblage – composed of echinoderms, bivalves, gastropods, serpulids and ostracods – did not significantly change during the deposition of unit 4, with the exception of bioturbation and some gastropod accumulations. The occurrence of large-sized gastropods at the base of subunit 4a suggests unstressed marine conditions. Interestingly, it reinforces the previous assertion that a putative Lilliput effect on gastropods was non-effective or overestimated, at least during the Smithian (Brayard *et al.* 2010, 2011*a*). Bioturbation seems more intense in subunits 4a and 4b compared to lithological unit 3. However, the quality of the outcrop did not allow us to adequately quantify the intensity of bioturbation in this latter unit. Below the fair-weather wave base, deposits of lithological unit 4 display dense, deep and large burrows that affect the entire thickness of the beds (Fig. 9). Colonization by bottom dwellers occurred at several stratigraphic horizons in the same bed. This suggests that successive generations of colonization reflect primary population density and are not linked to an important and long phase of sediment starvation. Although this dense ichnoassemblage is apparently not diversified (*Arenicolites* and *Palaeophycus* or *Planolites*), it is rather unusual not only for the Smithian but also for the entire Early Triassic. It does not entirely fit within traditional models of benthic recovery after the Permian–Triassic mass extinction that assume a progressive reappearance of dense, deep and large burrows only in the Spathian (e.g. Twitchett, 2006; but see Hofmann *et al.* 2011, 2013 for alternative models). Indeed, this type of ichnoassemblage within a subtidal setting is more in agreement with the concept of a

https://doi.org/10.1017/S0016756813000988 Published online by Cambridge University Press

shallow 'habitable zone' as proposed by Beatty, Zonneveld & Henderson (2008). Overall, it may indicate that environmental conditions were suitable for life (e.g. no anoxia) and stable. It also suggests that nutrients were profusely available during the deposition of these bioturbated beds.

8. Conclusion

Stacking patterns and geometric surfaces observed at Timpoweap Canyon reveal three different orders of relative sea-level fluctuations and high-frequency shoreline migrations. During the transition from Permian to Triassic, regional tectonic uplift related to the Sonoma Orogeny led to the deposition of terrigenous sediments of the Rock Canyon Conglomerate Formation. The first marine incursion, related to third-order sea-level transgression, occurred during the middle Smithian with deposition of limestones of the Sinbad Formation. A truncated surface at the top of the fenestral-microbial Sinbad limestones reflects a sudden sea-level drop, suggesting a tectonic influence still active in the Early Triassic. Inherited topographic highs of restricted local extension led to a different number of depositional sequences being recorded, according to the position along the coastline. Such limited geographic extension of some depositional sequences may distort our knowledge of delayed recovery of complex benthic communities after the end-Permian extinction. These small-scale, possibly climatically driven, depositional sequences resulted from shoreline migrations in excess of a few tens of metres and from sea-level drop and rise at a scale of 1–2 m.

The reconstruction of depositional settings in the Early Triassic of Timpoweap Canyon reflects the evolution of coastline sedimentation. Overlying the Permian–Triassic transition, alluvial fans and braided plains represent continental environments. The observed lateral facies variations indicate a progressive evolution from continental deposits to fenestral-microbial limestones in peritidal domain, and then to shallow subtidal marine environments with bivalves, gastropods, serpulids and echinoderms. Such a lateral facies variation highlights the control of the depositional setting upon the distribution of organisms. It also questions the anachronistic character of Early Triassic microbialites in the western USA basin.

Acknowledgements. The Région Bourgogne and the CNRS INSU Interrvie jointly supported this study. This is also a contribution to the ANR-funded project AFTER (ANR-13-JS06-0001-01). R. Hofmann and N. Goudemand (Zurich) are thanked for their help in ichnofossil and conodont determinations, respectively. D. Stephen is grateful for the ongoing financial support of the College of Science & Health at Utah Valley University. The studied outcrop is located on US public land under the stewardship of the Bureau of Land Management (BLM) of the US Department of the Interior; their management and access to these lands is much appreciated. S. Lucas and an anonymous reviewer provided constructive suggestions that helped us to improve the manuscript.

References

Baud, A., Richoz, S. & Pruss, S. B. 2007. The Lower Triassic anachronistic carbonate facies in space and time. *Global and Planetary Change* **55**, 81–9.

Beatty, T. W., Zonneveld, J.-P. & Henderson, C. M. 2008. Anomalously diverse Early Triassic ichnofossil assemblages in northwest Pangea: a case for a shallow-marine habitable zone. *Geology* **36**, 771–4.

Berra, F., Balini, M., Levera, M., Nicora, A. & Salamati, R. 2012. Anatomy of carbonate mounds from the Middle Anisian of Nakhlak (Central Iran): architecture and age of a subtidal microbial-bioclastic carbonate factory. *Facies* **58**, 685–705.

Blakey, R. C. 1974. Stratigraphic and depositional analysis of the Moenkopi Formation, southeastern Utah. *Utah Geological and Mineral Survey, Bulletin* **104**, 81 pp.

Blakey, R. C. 1977. Petroliferous lithosomes in the Moenkopi Formation, southern Utah. *Utah Geology* **4**, 67–84.

Blakey, R. C. 1979. Oil impregnated carbonate rocks of the Timpoweap Member, Moenkopi Formation, Hurricane Cliffs area, Utah and Arizona. *Utah Geology* **6**, 45–54.

Brayard, A., Bylund, K. G., Jenks, J., Stephen, D. A., Olivier, N., Escarguel, G., Fara, E. & Vennin, E. 2013. Smithian ammonoid faunas from Utah: implications for Early Triassic biostratigraphy, correlations and basinal paleogeography. *Swiss Journal of Paleontology* **132**, 141–219.

Brayard, A., Nützel, A., Kaim, A., Escarguel, G., Hautmann, M., Stephen, D. A., Bylund, K. G., Jenks, J. & Bucher, H. 2011*a*. Gastropod evidence against the Early Triassic Lilliput effect: Reply. *Geology* **39**, e233 pp.

Brayard, A., Nützel, A., Stephen, D. A., Bylund, K. G., Jenks, J. & Bucher, H. 2010. Gastropod evidence against the Early Triassic Lilliput effect. *Geology* **38**, 147–50.

Brayard, A., Vennin, E., Olivier, N., Bylund, K. G., Jenks, J., Stephen, D. A., Bucher, H., Hofmann, R., Goudemand, N. & Escarguel, G. 2011*b*. Transient metazoan reefs in the aftermath of the end-Permian mass extinction. *Nature Geoscience* **4**, 693–7.

Brühwiler, T., Bucher, H., Brayard, A. & Goudemand, N. 2010. High-resolution biochronology and diversity dynamics of the Early Triassic ammonoid recovery: The Smithian faunas of the Northern Indian Margin. *Palaeogeography, Palaeoclimatology, Palaeoecology* **297**, 491–501.

Chen, Z. Q., Fraiser, M. L. & Bolton, C. 2012. Early Triassic trace fossils from Gondwana Interior Sea: implication for ecosystem recovery following the end-Permian mass extinction in south high-latitude region. *Gondwana Research* **22**, 238–55.

Collinson, J. W., Kendall, C. G. S. C. & Marcantel, J. B. 1976. Permian-Triassic boundary in eastern Nevada and west-central Utah. *Bulletin of the Geological Society of America* **87**, 821–4.

Dickinson, W. R. 2006. Geotectonic evolution of the Great Basin. *Geosphere* **2**, 353–68.

Embry, A. F. 1997. Global sequence boundaries of the Triassic and their identification in the western Canada sedimentary basin. *Canadian Petroleum Geology Bulletin* **45**, 415–33.

ESTEBAN, M. & PRAY, L.C. 1983. Pisoids and pisolite facies (Permian), Guadalupe Mountains, New Mexico and West Texas. In *Coated Grains* (ed. T. Peryt), pp. 503–37. Berlin: Springer-Verlag.

FLÜGEL, E. 2004. Microfacies of carbonate rocks. Analysis, interpretation and application. Berlin, Heidelberg, New York: Springer, 976 pp.

FOREL, M.-B., CRASQUIN, S., KERSHAW, S. & COLLIN, P.-Y. 2013. In the aftermath of the end-Permian extinction: the microbialite refuge? *Terra Nova* **25**, 137–43.

FRAKES, L. A., FRANCIS, J. E. & SYKTUS, J. I. 1992. *Climate Modes of the Phanerozoic: The History of the Earth's Climate Over the Past 600 million Years*. Cambridge: Cambridge University Press, 274 pp.

GOODSPEED, T. H. & LUCAS, S. G. 2007. Stratigraphy, sedimentology, and sequence stratigraphy of the Lower Triassic Sinbad Formation, San Rafael Swell, Utah. In *Triassic of the American West* (eds S. G. Lucas & J. A. Spielmann), pp. 91–102. New Mexico Museum of Natural History and Science Bulletin no. 40.

GREGORY, H. E. 1950. Geology and geography of the Zion Park Region, Utah and Arizona. *Geological Survey Professional Paper* **220**, 1–200.

HALLAM, A. & WIGNALL, P. B. 1999. Mass extinctions and sea-level changes. *Earth Science Reviews* **48**, 217–50.

HAQ, B. U. & AL-QAHTANI, A. M. 2005. Phanerozoic cycles of sea-level change on the Arabian Platform. *Geoarabia* **10**, 127–60.

HAQ, U. B., HARDENBOL, J. & VAIL, P. R. 1987. Chronology of fluctuating sea levels since the Triassic. *Science* **235**, 1156–67.

HAQ, B. U. & SHUTTER, S. R. 2008. A chronology of Paleozoic sea-level changes. *Science* **322**, 64–8.

HEYDARI, E., HASSANZADEH, J., WADE, W. J. & GHAZI, A. M. 2003. Permian–Triassic boundary interval in the Abadeh section of Iran with implications for mass extinction: Part 1. Sedimentology. *Palaeogeography, Palaeoclimatology, Palaeoecology* **193**, 405–23.

HOFMANN, R., GOUDEMAND, N., WASMER, M., BUCHER, H. & HAUTMANN, M. 2011. New trace fossil evidence for an early recovery signal in the aftermath of the end-Permian mass extinction. *Palaeogeography, Palaeoclimatology, Palaeoecology* **310**, 216–26.

HOFMANN, R., HAUTMANN, M., WASMER, M. & BUCHER, H. 2013. Palaeoecology of the Spathian Virgin Formation (Utah, USA) and its implications for the Early Triassic recovery. *Acta Palaeontologica Polonica* **58**, 149–73.

HUANG, C., TONG, J., HINNOV, L. & CHEN, Z. 2011. Did the great dying of life take 700 k.y.? Evidence from global astronomical correlation of the Permian-Triassic boundary interval. *Geology* **39**, 779–82.

JENSON, J. 1986. Stratigraphy and facies analysis of the Upper Kaibab and Lower Moenkopi formations in Southwest Washington County, Utah. *Brigham Young University Geology Studies* **33**, 1–21.

KELLEY, N. P., MOTANI, R., JIANG, D. Y., RIEPPEL, O. & SCHMITZ, L. 2013. Selective extinction of Triassic marine reptiles during long-term sea-level changes illuminated by seawater strontium isotopes. *Palaeogeography, Palaeoclimatology, Palaeoecology*, published online 3 August 2012. doi: 10.1016/j.palaeo.2012.07.026.

KERSHAW, S., CRASQUIN, S., LI, Y., COLLIN, P.-Y., FOREL, M.-B., MU, X., BAUD, A., WANG, Y., XIE, S., MAURER, F. & GUO, L. 2012. Microbialites and global environmental change across the Permian-Triassic boundary: a synthesis. *Geobiology* **10**, 25–47.

KERSHAW, S., LI, Y., CRASQUIN-SOLEAU, S., FENG, Q., MU, X., COLLIN, P.-Y., REYNOLDS, A. & GUO, L. 2007. Earliest Triassic microbialites in the South China block and other areas: controls on their growth and distribution. *Facies* **53**, 409–25.

KIDDER, D. L. & WORSLEY, T. R. 2004. Causes and consequences of extreme Permo-Triassic warming to globally equable climate and relation to the Permo-Triassic extinction and recovery. *Palaeogeography, Palaeoclimatology, Palaeoecology* **203**, 207–37.

KONSTANTINOV, A.G. 2008. Triassic ammonoids of Northeast Asia: diversity and evolutionary stages. *Stratigraphy and Geological Correlation* **16**, 490–502.

LEHRMANN, D. J., PAYNE, J. L., PEI, D., ENOS, P., DRUKE, D., STEFFEN, K., ZHANG, J., WEI, J., ORCHARD, M. J. & ELLWOOD, B. 2007. Record of the End-Permian extinction and Triassic biotic recovery in the Chongzuo-Pingguo platform, southern Nanpanjiang basin, Guangxi, south China. *Palaeogeography, Palaeoclimatology, Palaeoecology* **252**, 200–17.

LUCAS, S. G., KRAINER, K. & MILNER, A. R. 2007. The type section and age of the Timpoweap Member and stratigraphic nomenclature of the Triassic Moenkopi Group in Southwestern Utah. In *Triassic of the American West* (eds S. G. Lucas & J. A. Spielmann), pp. 109–17. New Mexico Museum of Natural History and Science Bulletin no. 40.

MARENCO, P. J., GRIFFIN, J. M., FRAISER, M. L. & CLAPHAM, M. E. 2012. Paleoecology and geochemistry of Early Triassic (Spathian) microbial mounds and implications for anoxia following the end-Permian mass extinction. *Geology* **40**, 715–8.

MATA, S. A. & BOTTJER, D. J. 2011. Origin of Lower Triassic microbialites in mixed carbonate-siliciclastic successions: ichnology, applied stratigraphy, and the end-Permian mass extinction. *Palaeogeography, Palaeoclimatology, Palaeoecology* **300**, 158–178.

MCKEE, E. D. 1954. *Stratigraphy and History of the Moenkopi Formation of Triassic Age*. Geological Society of America, Memoir 61, 133 pp.

NIELSON, R. L. 1991. Petrology, sedimentology and stratigraphic implications of the Rock Canyon conglomerate, southwestern Utah. Utah Geological Survey, Miscellaneous Publication **91**, 1–65.

PAULL, R. A. & PAULL, R. K. 1993. Interpretation of Early Triassic nonmarine-marine relations, Utah, USA. *New Mexico Museum of Natural History and Science Bulletin* **3**, 403–9.

PAULL, R. K. & PAULL, R. A. 1997. Transgressive conodont faunas of the early Triassic: an opportunity for correlation in the Tethys and the circum-Pacific. In *Late Palaeozoic and Early Mesozoic Circum-Pacific Events and their Global Correlation* (eds J. M. Dickins, Y. Zunyi, Y. Hongfu, S. G. Lucas & S. K. Acharyya), pp. 158–67. Cambridge University Press, World and Regional Geology 10.

PÉREZ-LÓPEZ, A. & PÉREZ-VALERA, F. 2011. Tempestite facies model for the epicontinental Triassic carbonates of the Betic Cordillera (southern Spain). *Sedimentology* **59**, 646–78.

PERYT, T. M. 1983. Vadoids. In *Coated Grains* (ed. T. M. Peryt), pp. 437–49. Berlin, Heidelberg, New York: Springer.

PRUSS, S. B. & BOTTJER, D. J. 2004. Late Early Triassic microbial reefs of the western United States; a description and model for their deposition in the aftermath of the end-Permian mass extinction. *Palaeogeography, Palaeoclimatology, Palaeoecology* **211**, 127–37.

PRUSS, S. B., BOTTJER, D. J., CORSETTI, F. A. & BAUD, A. 2006. A global marine sedimentary response to the

end-Permian mass extinction: examples from southern Turkey and the western United States. *Earth-Science Reviews* **78**, 193–206.

QUIQUEREZ, A. & DROMART, G. 2006. Environmental control on granular clinoforms of ancient carbonate shelves. *Geological Magazine* **143**, 343–65.

REESIDE, J. B., JR. & BASSLER, H. 1922. Stratigraphic sections in southwestern Utah and northwestern Arizona. US Geological Survey, Professional Paper 129-D, pp. 53–77.

RIDENTE, D., PETRUNGARO, R., FALESE, F. & CHIOCCI, F. L. 2012. Middle–Upper Pleistocene record of 100-ka depositional cycles on the Southern Tuscany continental margin (Tyrrhenian Sea, Italy). Sequence architecture and margin growth pattern. *Marine Geology* **326–8**, 1–13.

ROMANO, C., GOUDEMAND, N., VENNEMANN, T. W., WARE, D., SCHNEEBELI-HERMANN, E., HOCHULI, P. A., BRÜHWILER, T., BRINKMANN, W. & BUCHER, H. 2013. Climatic and biotic upheavals following the end-Permian mass extinction. *Nature Geoscience* **6**, 57–60.

RUBAN, D. A. 2008. Evolutionary rates of the Triassic marine macrofauna and sea-level changes: Evidences from the Northwestern Caucasus, Northern Neotethys (Russia). *Palaeoworld* **17**, 115–25.

RUDDIMAN, W. F. 2003. Orbital insolation, ice volume, and greenhouse gases. *Quaternary Science Reviews* **22**, 1597–629.

SANO, H. & NAKASHIMA, K. 1997. Lowermost Triassic (Griesbachian) microbial bindstone-cementstone facies, southwest Japan. *Facies* **36**, 1–24.

SANO, H., ONOUE, T., ORCHARD, M. J. & MARTINI, R. 2012. Early Triassic peritidal carbonate sedimentation on a Panthalassan seamount: the Jesmond succession, Cache Creek Terrane, British Columbia. *Facies* **58**, 113–30.

SCHUBERT, J. K. & BOTTJER, D. J. 1992. Early Triassic stromatolites as post-mass extinction disaster forms. *Geology* **20**, 883–6.

SHACKLETON, N. J. 1987. Oxygen isotopes, ice volume and sea level. *Quaternary Science Reviews* **6**, 183–90.

STEWART, J. H., POOLE, F. G. & WILSON, R. F. 1972. Stratigraphy and origin of the Triassic Moenkopi Formation and related strata in the Colorado Plateau region. *Geological Survey Professional Paper* **691**, 1–195.

TWITCHETT, R. J. 2006. The palaeoclimatology, palaeoecology and palaeoenvironmental analysis of mass extinction events. *Palaeogeography, Palaeoclimatology, Palaeoecology* **232**, 190–213.

WEIDLICH, O. 2007. PTB mass extinction and earliest Triassic recovery overlooked? New evidence for a marine origin of Lower Triassic mixed carbonate–siliciclastic sediments (Rogenstein Member), Germany. *Palaeogeography, Palaeoclimatology, Palaeoecology* **252**, 259–69.

WOODS, A. D. 2009. Anatomy of an anachronistic carbonate platform: Lower Triassic carbonates of the southwestern United States. *Australian Journal of Earth Sciences* **56**, 825–39.

WOODS, A. D. 2013. Microbial ooids and cortoids from the Lower Triassic (Spathian) Virgin Limestone, Nevada, USA: evidence for an Early Triassic microbial bloom in shallow depositional environments. *Global and Planetary Change* **105**, 91–101.

WU, H., ZHANG, S., FENG, Q., JIANG, G., LI, H. & YANG, T., 2012. Milankovitch and sub-Milankovitch cycles of the early Triassic Daye Formation, South China and their geochronological and paleoclimatic implications. *Gondwana Research* **22**, 748–59.

YANG, H., CHEN, Z. Q., WANG, Y., TONG, J., SONG, H. & CHEN, J. 2011. Composition and structure of microbialite ecosystems following the End-Permian mass extinction in South China. *Palaeogeography, Palaeoclimatology, Palaeoecology* **308**, 111–28.

YANG, W. & LEHRMANN, D. J. 2003. Milankovitch climatic signals in Lower Triassic (Olenekian) peritidal carbonate successions, Nanpanjiang Basin, South China. *Palaeogeography, Palaeoclimatology, Palaeoecology* **201**, 283–306.

ZATOŃ, M., TAYLOR, P. D. & VINN, O. 2013. Early Triassic (Spathian) post-extinction microconchids from Western Pangea. *Journal of Paleontology* **87**, 159–65.

ZONNEVELD, J.-P., GINGRAS, M. K. & BEATTY, T. W. 2010. Diverse ichnofossil assemblages following the P-T mass extinction, Lower Triassic, Alberta and British Columbia, Canada: evidence for shallow marine refugia on the northwestern coast of Pangaea. *Palaios* **25**, 368–92.